O-D . . . O deuteron intra- and interbond exchange and frequency-dependent order parameter in deuteron glasses studied by two-dimensional exchange NMR

J. Dolinšek, B. Zalar, and R. Blinc
Jozef Stefan Institute, University of Ljubljana, Ljubljana, Slovenia
(Received 8 December 1993)

The question of whether the deuteron glass transition is an equilibrium phase transition or a metastable kinetic phenomenon, observed because of the finite experimental observation time, is addressed. Two-dimensional (2D) exchange NMR of O-D . . . O deuterons in deuteron glasses provides a unique possibility of a direct determination of the O-D . . . O intra- and interbond exchange times as well as for a determination of the Edwards-Anderson order parameter deeply in the glassy phase where 1D NMR methods for order parameter determination fail. On the frequency observation scales of spin-lattice relaxation and line-shape studies 10^3–10^8 Hz, the deuteron glass phase appears static. 2D exchange NMR extends the frequency observation window into the mHz region. The O-D . . . O deuteron intrabond exchange time τ_{exch} in $Rb_{0.68}(ND_4)_{0.32}D_2AsO_4$ has been determined as a function of temperature below 45 K. A very slow fluctuation in the H-bond double minimum potential is detected which averages out the H-bond asymmetry and the glass order parameter to zero at long-enough times. The deuteron glass phase is nonergodic, showing a frozen-in disorder at times $t \ll \tau_{exch}$, whereas for times long compared to τ_{exch}, ergodicity is restored.

I. INTRODUCTION

The physics of glasses remains one of the great unsolved problems of condensed-matter physics. The basic open question is whether we deal with a phase transition to a new kind of a thermodynamic state or whether the tremendous slowing down of the structural rearrangement time in glasses is just a kinetic phenomenon and the observed freezing is due to a finite observation time of experimental measuring techniques.

One possible answer to this problem has been obtained for the case of magnetic spin glasses. Here Edwards and Anderson[1] introduced a well-defined statistical model leading to an ergodic-nonergodic phase transition with local freezing but without long-range ordering. Sherrington and Kirkpatrick[2] introduced an infinite-range version of this model which has been exactly solved by Parisi.[3] Here the low-temperature phase consists of an infinite number of pure states characterized by an infinite number of order parameters. The slow response of these systems below the glass transition temperature is believed to be due to the fact that the free-energy surface in microscopic parameter phase space has a highly fractal mountain landscape, with high barriers separating regions which behave as long-lived phases, and an ultrametric overlap structure. Below the spin-glass transition the system becomes nonergodic and gets trapped into these pure states. In an external magnetic field the phase transition is not destroyed as in case of ferromagnets. In the magnetic-field–temperature plane there is a line of phase transitions known as de Almeida–Thouless line,[4] below which the paramagnetic phase becomes unstable.

On the experimental side, evidence for an equilibrium phase transition in spin glasses is still inconclusive. The measurement of field-cooled (fc) and zero-field-cooled (zfc) magnetic susceptibilities[5,6] indicates that the establishment of full thermal equilibrium is a delicate matter. The distinction between fc and zfc susceptibilities below the freezing temperature T_f depends on the cooling rate and the fc magnetization slowly changes with time. The zfc susceptibility, on the other hand, depends strongly on the time the sample is kept at constant temperature after cooling prior to field application. According to this, some authors conclude that the spin-glass state is a nonequilibrium one, in the thermodynamical sense.

It is not absolutely certain that the above results prove the nonequilibrium character of the spin-glass state. If states with a spin-glass order exist as thermal equilibrium states, they are certainly highly degenerate, with many order-parameter components. On cooling, the system would form ordered regions of its various possible order-parameter components below T_f. As these regions grow, there would be misfit at their walls and hence the growth of domains might be extremely slow. In view of this alternative possible interpretation of some of the experimental findings, the existence of a unique static freezing temperature T_f was studied.[7] A frequency-dependent freezing temperature $T_f(\omega)$ has been determined from the magnetic susceptibility maximum. The frequency dependence of $T_f(\omega)$ over the observed frequency range was however rather weak, so that the $\omega \rightarrow 0$ limit could not discriminate whether $T_f(\omega \rightarrow 0)$ approaches zero absolute temperature or it actually settles down to a nonzero static value.

Some evidence for an equilibrium phase transition has been obtained from the measurement of the nonlinear susceptibility, which is more sensitive to spin-glass order than the zero-field susceptibility. Various authors[6] show that the observed power-law divergence at the freezing temperature is consistent with the appearance of a thermodynamic phase transition. As shown later,[6] the data

0163-1829/94/50(2)/805(17)/$06.00

are not completely conclusive in the vicinity of T_f, where they can be fitted with a rather arbitrary exponent and there can be as well some ambiguities due to sample inhomogeneities on large scales.

All the above experiments have in common that the data are probably affected by the finite measurement frequency interval or finite observation time of the applied measuring technique. This is due to the fact that the spectrum of correlation times for internal motions in spin glasses as well as in other types of glasses is very broad. The correlation times cover the range from extremely short times up to the age of the universe.

In structural glasses such as H-bonded proton and deuteron glasses the situation is even less clear. Here the Sherrington-Kirkpatrick model has been extended[8] to describe the frozen proton pseudospin-glass (PG) phase observed in the mixed hydrogen-bonded ferro- and antiferroelectric crystals such as $Rb_{1-x}(NH_4)_xH_2PO_4$, commonly abbreviated as RADP. In analogy to spin glasses, the frozen PG state is believed to be due to quenched random interactions between the pseudospin degrees of freedom, which represent the two equilibrium positions of the protons within the O-H. . . O bond. The model was further refined by introducing an effective local random field.[9] This field makes the H bonds asymmetric and is the consequence of the random substitutional disorder of Rb^+ and $(NH_4)^+$ ions in the host crystal lattice. In the random field variance-temperature plane there exists a de Almeida–Thouless-like line, separating the ergodic phase, described by a single order parameter of the Edwards-Anderson type q_{EA}, from the nonergodic phase, described by an infinite number of order parameters. The essential difference between the magnetic spin glasses and the proton pseudospin glasses is the fact that in the latter an intrinsic random field, generated by substitutional impurities, always exists and its presence adds new features to the PG case. Thus, PG is not just another analog of the magnetic spin glass. This random field smears out the PG transition and the onset of ordering of hydrogens in the H-bonds takes place already at temperatures high above the nominal glass temperature T_G. Isotopic substitution of protons with deuterons drastically reduces the tunneling frequency and shifts the formation of a deuteron glass (DG) phase towards higher temperatures.

The experimental verification of the existence of a phase transition in proton glasses is still far from being conclusive. Experimental determination of the field-cooled and zero-field-cooled static dielectric susceptibilities of the deuteron glass $Rb_{0.4}(ND_4)_{0.6}D_2PO_4$ has shown[10] that above the freezing temperature T_f the two susceptibilities are equal, whereas the splitting of the two branches and a remnant polarization is observed below T_f. The splitting may demonstrate the occurrence of an ergodic-nonergodic transition on crossing the de Almeida–Thouless-like line. Repeating the experiment with an ac field of different frequencies in the range 0.1–0.001 Hz has shown[11] that the temperature, where the splitting of fc and zfc susceptibilities occurs, is frequency dependent, $T_f = T_f(\omega)$. $T_f(\omega)$ was decreasing with a decreasing ω. The observed value of the freezing temperature thus depends on the experimental time scale, suggesting that the freezing process is a dynamical phenomenon. As one approaches the freezing transition, the maximum relaxation time is expected to diverge at the Vogel-Fulcher temperature T_0. T_0 thus corresponds to the static freezing temperature $T_f(\omega=0)$ which may be, in principle, observed in a static experiment on an infinite time scale.

On the NMR line shape[12–16] and spin-lattice relaxation time scale a perfectly static frozen-in disorder of the local H-bond polarizations has been found. The Edwards-Anderson order parameter q_{EA} has been determined in a large temperature interval and its temperature dependence found to agree with the Pirc-Tadić-Blinc[9] (PTB) model. It has been shown that q_{EA} is nonzero already far above the nominal glass transition temperature T_G, which was found in $Rb_{0.56}(ND_4)_{0.44}D_2PO_4$ to be around 85 K. This demonstrated the predicted random-field smearing of the glass transition from the paraelectric to the ergodic PG phase. q_{EA} could be determined from the second moment M_2 of the quadrupole perturbed Zeeman absorption line. q_{EA}, which is conjugate to the variance of the random field, measures the order of an ergodic system effectively locked in one of the global or side minima of the fractal mountainlike free-energy surface in the phase space. At lower temperatures the system is expected to become nonergodic and the single order parameter q_{EA} should be replaced by an order-parameter distribution function[3] $q(x)$. No attempt to discriminate between q_{EA} and $q(x)$ from NMR data has been successful so far.[13]

The determination of q_{EA} from the NMR experimental data thus allows for the possibility that the glassy disorder in H-bonded systems like RADP is completely static, so that we are dealing with an equilibrium phase transition. It should be, however, kept in mind that the observation window of the NMR line-shape measuring technique lies in the kHz region. To test the above conclusion, it is necessary to extend the observation window of NMR towards lower frequencies by several orders of magnitude. Such an extension is possible by the application of two-dimensional (2D) "exchange" NMR spectroscopy. Here one can correlate a certain state of the investigated system in two distinct instants of time, separated by a certain time interval. Since the same state is monitored in two successive times in a coherent manner, one can detect the internal motions, which have time constants as slow as is the time separation between the two observations of the system. The separation time interval is called the mixing time. It can be as long as the spin-lattice relaxation time. Since the latter in DRADP mixtures amounts to several hundred seconds for deuteron nuclei at temperatures below 50 K, the observation window of 2D exchange technique falls in the Milli-Hertz region. The application of this technique should thus elucidate, whether the frozen-in glass disorder—as seen by the NMR line-shape analysis—is a true equilibrium state of the system, or it only appears static because of the finite observation window of the measurement technique. In addition such measurements yield information on the local dynamics of deuteron glasses which has not been systematically studied so far. Site-specific dynamic mea-

surements, in particular, can determine whether the O-D. . . O deuterons are indeed the basic two-position reorientable dipoles in deuteron glasses as assumed by the PTB (Ref. 9) model or not.

II. TWO-DIMENSIONAL EXCHANGE NMR OF DEUTERONS IN H-BONDED SYSTEMS

Two-dimensional exchange NMR of nuclei with spin $I=1$ has been considered in detail by Spiess and coworkers.[17,18] The basic pulse sequence consists of four pulses [Fig. 1(a)]. The preparation pulse ψ creates transverse magnetization, which precesses freely in the evolution period, characterized by the time variable t_1. The second pulse ϕ stores the information on the spin precession angle during t_1 into the longitudinal magnetization. In the mixing period, characterized by the time interval τ_m, the spin magnetization is aligned along the magnetic field and is subjected to spin-lattice relaxation. The mixing period is normally much longer than any other period in the 2D exchange experiment. If chemical exchange takes place during that period, the nucleus changes its chemical environment, resulting in a different local precession frequency. This difference for spin $I=1$ mainly arises from the change in the electric-field-gradient (EFG) tensor. One can say that during the mixing period the nucleus has changed its Hamiltonian. At the end of the mixing period a two-pulse detection scheme, with pulses separated by a time τ, is applied. The acquisition of the signal is made in the detection period, with the time variable labeled t_2. In this period the spin system precesses freely with the frequency, corresponding to the new Hamiltonian. In the case that the exchange is slow, taking place only during the extended mixing period, the signal is actually independent of the time τ and an undistorted line-shape results.[17] For fast exchange, taking place in all time intervals of the pulse sequence, the line shape is affected by the evolution in the time τ as well.[18] The coherence transfer pathway diagram[19] used to select the proper form of the signal is shown in Fig. 1(b). Here $p=M_m-M_n$ is the difference in magnetic quantum numbers of the two spin states $|m\rangle$ and $|n\rangle$, coupled by a given coherence. The above pathway is achieved by cycling the pulses ψ and ϕ in steps of π and α in steps of $\pi/2$. Pulse β is shifted for $\pm\pi/2$ from the phase of α.

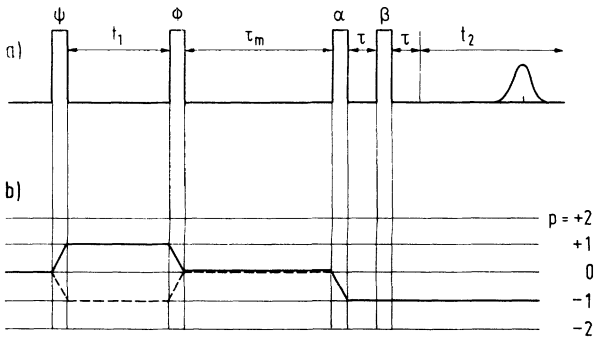

FIG. 1. (a) Pulse sequence for 2D exchange NMR of deuterons ($I=1$). (b) Coherence transfer pathway diagram following the phase cycling procedure of Table I.

TABLE I. Phase cycle of the four pulses and the receiver phase for 2D exchange experiment of spins with $I=1$.

ψ	ϕ	α	β	ϕ^{rec}
$+X$	$+X$	$+X$	$+Y$	$+X$
$-X$	$+X$	$+X$	$+Y$	$-X$
$+X$	$-X$	$+X$	$+Y$	$-X$
$-X$	$-X$	$+X$	$+Y$	$+X$
$+X$	$+X$	$+X$	$-Y$	$+X$
$-X$	$+X$	$+X$	$-Y$	$-X$
$+X$	$-X$	$+X$	$-Y$	$-X$
$-X$	$-X$	$+X$	$-Y$	$+X$
$+X$	$+X$	$+Y$	$-X$	$+Y$
$-X$	$+X$	$+Y$	$-X$	$-Y$
$+X$	$-X$	$+Y$	$-X$	$-Y$
$-X$	$-X$	$+Y$	$-X$	$+Y$
$+X$	$+X$	$+Y$	$+X$	$+Y$
$-X$	$+X$	$+Y$	$+X$	$-Y$
$+X$	$-X$	$+Y$	$+X$	$-Y$
$-X$	$-X$	$+Y$	$+X$	$+Y$
$+X$	$+X$	$-X$	$-Y$	$-X$
$-X$	$+X$	$-X$	$-Y$	$+X$
$+X$	$-X$	$-X$	$-Y$	$+X$
$-X$	$-X$	$-X$	$-Y$	$-X$
$+X$	$+X$	$-X$	$+Y$	$-X$
$-X$	$+X$	$-X$	$+Y$	$+X$
$+X$	$-X$	$-X$	$+Y$	$+X$
$-X$	$-X$	$-X$	$+Y$	$-X$
$+X$	$+X$	$-Y$	$+X$	$-Y$
$-X$	$+X$	$-Y$	$+X$	$+Y$
$+X$	$-X$	$-Y$	$+X$	$+Y$
$-X$	$-X$	$-Y$	$+X$	$-Y$
$+X$	$+X$	$-Y$	$-X$	$-Y$
$-X$	$+X$	$-Y$	$-X$	$+Y$
$+X$	$-X$	$-Y$	$-X$	$+Y$
$-X$	$-X$	$-Y$	$-X$	$-Y$

The appropriate receiver phase shift (Table I) is also applied. The Cyclops phase cycle for elimination of the quadrature detection errors is inherent in that cycle. The above cycle selects the signal of the form

$$F_{cc} \propto \cos\omega^{(e)}t_1 \cos\omega^{(d)}t_2 e^{-\tau_m/T_1} . \quad (1)$$

Here $\omega^{(e)}$ is the absorption frequency, corresponding to the nuclear spin Hamiltonian of the evolution period and $\omega^{(d)}$ is the frequency of the detection period Hamiltonian. When no chemical exchange takes place, $\omega^{(e)}=\omega^{(d)}$ and the absorption peak lies on the diagonal of the 2D spectrum. If chemical exchange between two physically nonequivalent sites has occurred, the peak lies at the cross position $(\omega^{(e)},\omega^{(d)})$ in the 2D spectrum, with $\omega^{(e)}\neq\omega^{(d)}$. The amplitude of the signal given by Eq. (1) is the largest when the length of all four pulses is 90°.

III. EXCHANGE IN AN ASYMMETRIC TWO-SITE POTENTIAL

In hydrogen-bonded systems, like deuterated DRADP, acid deuterons are located in the O-D. . . O bonds. It has been shown[20] that interbond exchange of deuterons between different H bonds is completely frozen already far above the onset of the glass phase, so that only the intra-

bond O-D. . . O exchange results in pseudospin reversal. A given H bond is represented by a double minimum potential (Fig. 2), with A and B describing the two possible locations of the deuteron in the bond. In general, the H bond is asymmetric with an energy difference Δ between the two equilibrium sites. In the course of time, the deuteron can change its position $A \leftrightarrow B$ either by incoherent thermally activated jumps over the barrier or by a coherent quantum tunneling. In the following the term "exchange" will be used to describe the intrabond deuteron jumps. The two exchange rates satisfy the detailed balance conditions

$$K_{AB}=\Omega_0 e^{-\Delta/2kT}, \tag{2a}$$

$$K_{BA}=\Omega_0 e^{\Delta/2kT}, \tag{2b}$$

where $\Omega_0=\tau_{\text{exch}}^{-1}=(\tau_0 e^{E_a/kT})^{-1}$ is the jump frequency for the symmetric bond and the index AB denotes the jumps $A \rightarrow B$. We define a 2×2 population matrix W, the diagonal elements of which represent the equilibrium populations of the sites A and B:

$$W=\frac{1}{2\cosh(\Delta/2kT)}\begin{bmatrix} e^{\Delta/2kT} & 0 \\ 0 & e^{-\Delta/2kT} \end{bmatrix}. \tag{3}$$

Following the definitions of Spiess,[18] we write the NMR signal, produced by the pulse sequence of Fig. 1 for the general case, when the intrabond exchange can occur in any of the time intervals of the pulse sequence as

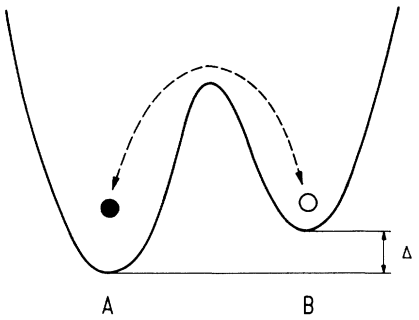

FIG. 2. A schematic representation of the asymmetric hydrogen-bond double-well potential.

$$F_{cc}(t_1,\tau_m,\tau,t_2)=\tfrac{1}{2}\text{Re}\{G_- + G_+\}. \tag{4}$$

The functions $G_\pm$ are written in the form

$$G_\pm(t_1,\tau_m,\tau,t_2) = \langle 1|\tilde{Q}_\pm(t_2)\tilde{Q}_\pm(\tau)\tilde{Q}_\mp(\tau)\tilde{K}_{1/1}(\tau_m)\tilde{Q}_+(t_1)W|1\rangle . \tag{5}$$

$|1\rangle$ is a two-component unit vector

$$|1\rangle=\begin{bmatrix}1\\1\end{bmatrix}. \tag{6}$$

The 2×2 matrix $\tilde{Q}_\pm(t)$ has a form

$$\tilde{Q}_\pm(t)=\frac{1}{2\eta}\exp\left[-t\left[\Omega_0\cosh\frac{\Delta}{2kT}\mp\frac{i(\omega_A+\omega_B)}{2}+\frac{1}{T_2}\right]\right]\begin{bmatrix}(\eta+\zeta)e^{-\eta t}+(\eta-\zeta)e^{\eta t} & \Omega_0 e^{\Delta/2kT}(e^{\eta t}-e^{-\eta t}) \\ \Omega_0 e^{-\Delta/2kT}(e^{\eta t}-e^{-\eta t}) & (\eta-\zeta)e^{-\eta t}+(\eta+\zeta)e^{\eta t}\end{bmatrix}. \tag{7}$$

Here T_2 is the spin-spin relaxation time and $\sigma=(\omega_B-\omega_A)/2$ is half the difference between the absorption frequencies of the A and B sites. The parameters ζ and η are

$$\zeta=\pm i\sigma-\Omega_0\sinh\frac{\Delta}{2kT}, \tag{8a}$$

$$\eta=\sqrt{\zeta^2+\Omega_0^2}. \tag{8b}$$

The matrix $\tilde{Q}_\pm(t)$ describes the free precession of spins as well as the exchange during precession. The exchange matrix $\tilde{K}_{1/1}(\tau_m)$ describes the exchange and spin-lattice relaxation during the mixing period:

$$\tilde{K}_{1/1}(\tau_m)=\frac{1}{2\cosh(\Delta/2kT)}\exp\left[-\frac{\tau_m}{T_1}\right]\begin{bmatrix} e^{\Delta/2kT}+e^{-\Delta/2kT}e^{-2\Omega_0\tau_m\cosh(\Delta/2kT} & e^{\Delta/2kT}(1-e^{-2\Omega_0\tau_m\cosh(\Delta/2kT)}) \\ e^{-\Delta/2kT}(1-e^{-2\Omega_0\tau_m\cosh(\Delta/2kT)}) & e^{-\Delta/2kT}+e^{\Delta/2kT}e^{-2\Omega_0\tau_m\cosh(\Delta/2kT)}\end{bmatrix}. \tag{9}$$

Here T_1 is the spin-lattice relaxation time which is taken to be the same for both sites of the double potential. The case when the relaxation rates $r_A=1/T_{1A}$ and $r_B=1/T_{1B}$ of the sites A and B differ is treated in Appendix A. The case when T_1 depends on the bond asymmetry Δ, describing a distribution of $T_1=T_1(\Delta)$, is treated in Appendix B.

In general the evolution and detection periods are of negligible duration in comparison to the mixing period. If exchange occurs only during mixing, one obtains the signal F_{cc} [Eq. (4)] in the form

$$F_{cc}(t_1,t_2,\tau_m)=e^{-\tau_m/T_1}e^{-(t_1+t_2)/T_2}\{a_{AA}(\tau_m)\cos\omega_A t_1\cos\omega_A t_2+a_{BB}(\tau_m)\cos\omega_B t_1\cos\omega_B t_2 + a_{AB}(\tau_m)\cos\omega_A t_1\cos\omega_B t_2+a_{BA}(\tau_m)\cos\omega_B t_1\cos\omega_A t_2\}, \tag{10}$$

where the assumption of an exponential decay of the signal has been made. The first two terms in the curly bracket of Eq. (10) give the diagonal peaks in the spectrum, whereas the last two terms give the cross peaks. The intensities $a_{ij}(\tau_m)$ are given by

$$a_{AA}(\tau_m)=\frac{1}{[2\cosh(\Delta/2kT)]^2}\left[e^{\Delta/kT}+e^{-2\Omega_0\tau_m\cosh(\Delta/2kT)}\right], \tag{11a}$$

$$a_{BB}(\tau_m)=\frac{1}{[2\cosh(\Delta/2kT)]^2}\left[e^{-\Delta/kT}+e^{-2\Omega_0\tau_m\cosh(\Delta/2kT)}\right], \tag{11b}$$

$$a_{AB}(\tau_m)=a_{BA}(\tau_m)=\frac{1}{[2\cosh(\Delta/2kT)]^2}\left[1-e^{-2\Omega_0\tau_m\cosh(\Delta/2kT)}\right]. \tag{11c}$$

The 2D spectrum is obtained by a 2D Fourier transformation

$$I_{cc}(\omega_1,\omega_2,\tau_m,\Delta)=\int_0^\infty\int_0^\infty F_{cc}(t_1,t_2,\tau_m,\Delta)e^{-i\omega_1 t_1}e^{-i\omega_2 t_2}dt_1dt_2\ , \tag{12}$$

where the dependence on the asymmetry of the H-bond Δ is explicitly emphasized. In the case that the exchange is not occurring during the mixing period only, the evolution of the signal [Eq. (4)] is not so simple and it is the best to treat it numerically.

We evaluate the diagonal and cross peak intensities [Eqs. (11a)–(11c)] in the limit of long mixing times $\Omega_0\tau_m \gg 1$ (taking $T_1\to\infty$):

$$a_{AA}(\infty)=\frac{1}{[2\cosh(\Delta/2kT)]^2}e^{\Delta/kT}, \tag{13a}$$

$$a_{BB}(\infty)=\frac{1}{[2\cosh(\Delta/2kT)]^2}e^{-\Delta/kT}, \tag{13b}$$

$$a_{AB}(\infty)=a_{BA}(\infty)=\frac{1}{[2\cosh(\Delta/2kT)]^2}. \tag{13c}$$

The assumption $T_1\to\infty$ is actually unnecessary since the quantities of interest will be the ratios between cross and diagonal peak intensities. In case that T_1 is independent of the deuteron sites A and B, i.e., one is dealing with a single constant T_1, the term involving T_1 appears as a common prefactor in the formulas for cross and diagonal peak intensities. In the calculation of the ratios, these terms cancel.

IV. EXCHANGE SPECTRUM IN THE GLASSY STATE

We apply now the results of the previous section to an ensemble of H bonds with a random distribution of bond asymmetries, forming a deuteron glass phase. The asymmetries are distributed with a distribution function $\rho(\Delta)$, which is symmetric,

$$\rho(\Delta)=\rho(-\Delta)\ , \tag{14}$$

and centered around $\Delta=0$. This accounts for the fact that in the glass phase there exists no macroscopic order of deuterons in the H bonds and the average polarization p of the bonds is zero,

$$\langle p\rangle=\langle W_A-W_B\rangle=\left\langle\tanh\frac{\Delta}{2kT}\right\rangle=0\ . \tag{15}$$

Here W_A and W_B represent the equilibrium populations of the two sites in the bond, given by the elements of the matrix W [Eq. (3)] and the average is made over all bonds in the crystal.

We average now the intensities [Eqs. (11a)–(11c)] over the distribution $\rho(\Delta)$. We make the definitions

$$x=\Omega_0\tau_m\ , \tag{16a}$$

$$u=\Delta/2kT\ , \tag{16b}$$

and use

$$\rho(\Delta)d\Delta=g(u)du\ . \tag{16c}$$

The intensities now become

$$\langle a_{AA}(x)\rangle=\frac{1}{4}\int_{-u_{\max}}^{u_{\max}}du\,g(u)\frac{e^{2u}}{\cosh^2u}+\frac{1}{4}\int_{-u_{\max}}^{u_{\max}}du\,g(u)\frac{e^{-2x\cosh u}}{\cosh^2u}\ , \tag{17a}$$

$$\langle a_{BB}(x)\rangle=\frac{1}{4}\int_{-u_{\max}}^{u_{\max}}du\,g(u)\frac{e^{-2u}}{\cosh^2u}+\frac{1}{4}\int_{-u_{\max}}^{u_{\max}}du\,g(u)\frac{e^{-2x\cosh u}}{\cosh^2u}\ , \tag{17b}$$

$$\langle a_{AB}(x)\rangle=\langle a_{BA}(x)\rangle=\frac{1}{4}\int_{-u_{\max}}^{u_{\max}}du\,g(u)\frac{1}{\cosh^2u}-\frac{1}{4}\int_{-u_{\max}}^{u_{\max}}du\,g(u)\frac{e^{-2x\cosh u}}{\cosh^2u}\ . \tag{17c}$$

Here we integrate on a symmetric interval between $\pm u_{\max}$, where $|u_{\max}|$ represents the maximum asymmetry of the double-well potential. Since $g(u)$ is symmetric, both diagonal peaks have equal intensities,

$$\frac{\langle a_{AA}(x)\rangle}{\langle a_{BB}(x)\rangle}=1\ . \tag{18a}$$

We define

$$I_a=\int_{-u_{\max}}^{u_{\max}}du\,g(u)\frac{e^{2u}}{\cosh^2u}\ , \tag{18b}$$

$$I_b(x)=\int_{-u_{\max}}^{u_{\max}}du\,g(u)\frac{e^{-2x\cosh u}}{\cosh^2u}\ , \tag{18c}$$

$$I_c=\int_{-u_{\max}}^{u_{\max}}du\,g(u)\frac{1}{\cosh^2u}\ , \tag{18d}$$

and write the ratio of the cross to diagonal peak intensities:

$$R(x)=\frac{\langle a_{BA}(x)\rangle}{\langle a_{AA}(x)\rangle}=\frac{I_c-I_b(x)}{I_a+I_b(x)}\ . \tag{18e}$$

Due to Eqs. (17c) and (18a) this ratio is the same for both pairs of cross and diagonal peaks: $\langle a_{BA}\rangle/\langle a_{AA}\rangle=\langle a_{AB}\rangle/\langle a_{BB}\rangle$.

Let us now consider first this ratio for the trivial case when all the bonds are symmetric. We take $g(u)=\delta(u)$ and label the ratio of the cross to diagonal peak intensities as $R_0(x)$. We get

$$I_a=I_c=1\ ,\quad I_b(x)=e^{-2x}\ ,$$

and

$$R_0(x)=\tanh x\ . \tag{19a}$$

The saturated value of this ratio for long mixing times ($x=\Omega_0\tau_m\rightarrow\infty$) is

$$R_0(\infty)=1\ . \tag{19b}$$

Next we consider the distribution $g(u)$, which has a certain width and is symmetric. This should properly describe the glass phase. We look for the asymptotic value of the ratio $R(x)$ for long mixing times $x\rightarrow\infty$. Here $I_b(\infty)=0$ and we have

$$R(\infty)=\frac{\langle a_{BA}(\infty)\rangle}{\langle a_{AA}(\infty)\rangle}=\frac{I_c}{I_a}=\frac{\int_{-u_{\max}}^{u_{\max}}du\,g(u)(1/\cosh^2u)}{\int_{-u_{\max}}^{u_{\max}}du\,g(u)(e^{2u}/\cosh^2u)}\ . \tag{20a}$$

We rewrite

$$\int_{-u_{\max}}^{u_{\max}}du\,g(u)\frac{e^{2u}}{\cosh^2u}=2\int_0^{u_{\max}}du\,g(u)\frac{\cosh 2u}{\cosh^2u}\ , \tag{20b}$$

and find the inequality

$$R(\infty)=\frac{\int_{-u_{\max}}^{u_{\max}}du\,g(u)(1/\cosh^2u)}{\int_{-u_{\max}}^{u_{\max}}du\,g(u)(\cosh 2u/\cosh^2u)}<1\ , \tag{20c}$$

since denominator is always larger than numerator.

This important result states the following: as soon as the glassy phase is characterized by a symmetric distribution of H-bond asymmetries with zero mean value, the saturated value of the ratio of cross peak to diagonal peak intensities will be less than one. It will become unity only in the limit when all individual H bonds are symmetric.

We can relate the ratio $R(\infty)$ to the Edwards-Anderson order parameter

$$q_{\rm EA}=\langle p^2\rangle\ , \tag{21a}$$

where $p=\tanh u$ and the average is taken over all bonds. We have

$$q_{\rm EA}=\int_{-u_{\max}}^{u_{\max}}du\,g(u)\tanh^2u=1-\int_{-u_{\max}}^{u_{\max}}du\,g(u)\frac{1}{\cosh^2u}\ , \tag{21b}$$

taking into account the fact that $g(u)$ is normalized to unity. For the ratio $R(\infty)$ we get

$$R(\infty)=\frac{1-q_{\rm EA}}{1+q_{\rm EA}}\ , \tag{22}$$

thus a nonzero value of $q_{\rm EA}$ immediately implies the ratio $R(\infty)$ to be less than one. Alternatively, the measured value of $R(\infty)$ could be used to determine $q_{\rm EA}$:

$$q_{\rm EA}=\frac{1-R(\infty)}{1+R(\infty)}\ . \tag{23}$$

A 2D NMR measurement of $R(\infty)$ thus allows for a determination of the Edwards-Anderson order parameter $q_{\rm EA}$ in the slow motion regime where the determination of $q_{\rm EA}$ from line-shape data[13] is no longer possible.

So far the asymmetry distribution function has not been specified explicitly. In the random-bond–random-field model[13] the distribution function of local polarization $W(p)$ has been derived, using the replica formalism.[8] For the replica symmetric phase an analytic result has been obtained:

$$W(p)=\frac{1}{\sqrt{2\pi Q^2}}\frac{1}{1-p^2}\exp\left[-\frac{\operatorname{arctanh}^2p}{2Q^2}\right]\ , \tag{24a}$$

with

$$Q=\frac{T_G}{T}\sqrt{q_{\rm EA}+\tilde{\Delta}}\ , \tag{24b}$$

where $q_{\rm EA}$ is determined from the self-consistent equation

$$q_{\rm EA}=\frac{1}{\sqrt{2\pi}}\int_{-\infty}^{\infty}dz\exp(-z^2/2)\times\tanh^2\left[\frac{T_G}{T}\sqrt{q_{\rm EA}+\tilde{\Delta}}z\right]\ . \tag{24c}$$

Here $T_G=J/k_B$ and $\tilde{\Delta}=\Delta/J^2$ are the glass transition temperature and the variance of the random field. The parameters J^2 and Δ specify the widths of the random-bond and random-field distributions.[9] Since $p=\tanh(\Delta/2kT)=\tanh u$ we can relate $W(p)$ to $g(u)$ via $W(p)dp=g(u)du$ and obtain

$$g(u)=\frac{1}{\sqrt{2\pi Q^2}}\exp\left[-\frac{u^2}{2Q^2}\right]\ , \tag{24d}$$

which is a Gaussian distribution of the asymmetries of the H bonds. In Fig. 3 the calculated ratio of cross peak to diagonal peak intensities $R(x)$, defined by Eq. (18e), is shown as a function of the normalized mixing time $x=\Omega_0\tau_m$ for different temperatures. The parameters $T_G=90$ K and $\tilde{\Delta}=0.35$ are taken from the O-D...O deuteron line-shape analysis[13] in $Rb_{0.56}(ND_4)_{0.44}D_2PO_4$ and the distribution function $g(u)$ of Eq. (24d) has been used. The main feature of the result—based on a completely static frozen-in disorder picture—is the appearance of a saturated value $R(\infty)$ which is less than unity and tends to zero, when the glass order parameter $q_{\rm EA}$ tends to one. $R(\infty)$ equals one only for the case that all individual H bonds are symmetric.

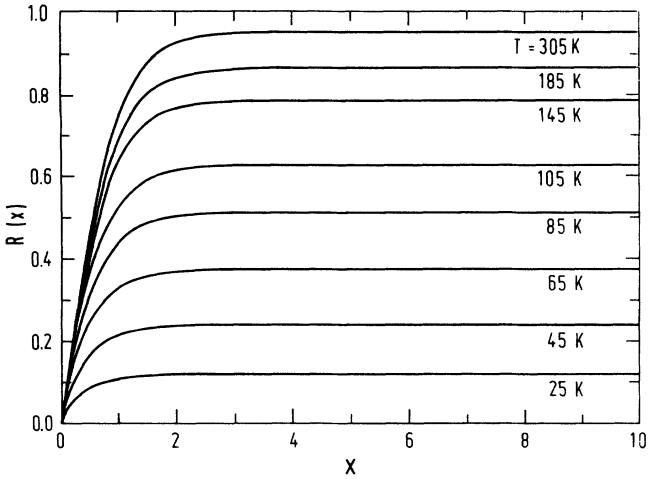

FIG. 3. The calculated ratio [Eq. (18e)] of the cross peak to diagonal peak intensities $R(x)$ as a function of the normalized mixing time $x=\Omega_0\tau_m$ for a static glass (random-bond–random-field Ising model) at different temperatures. The parameters $T_G=90$ K and $\tilde{\Delta}=0.35$ are taken from the line-shape analysis.

V. O-D... O DEUTERON INTRABOND EXCHANGE IN $Rb_{0.68}(ND_4)_{0.32}D_2AsO_4$

A 2D NMR experiment, showing an O-D... O intrabond exchange has been performed in $Rb_{0.68}(ND_4)_{0.32}D_2AsO_4$ (DRADA-32) at temperatures below 50 K. According to the line-shape analysis, the system is at these temperatures already deeply in the glass phase. A 1D O-D... O spectrum at an orientation $\mathbf{a}\perp\mathbf{H}_0, \angle\mathbf{c},\mathbf{H}_0=45°$, and $T=40$ K is shown in Fig. 4. The spectrum is symmetric around the dashed line, the left part corresponding to the $1\rightarrow0$ transitions and the right part to the $0\rightarrow1$ transitions. The H-bond network [Fig. 5(a)] lies in the X,Y plane and consists of two sets of mutually perpendicular chains of H bonds, linking together adjacent AsO_4 tetrahedra. The lines A and B correspond to the so-called X_+ and X_- bonds.[21] Here X stands for the direction of the bond chain. There are two kinds of X bonds because of the 0.5° angle between the direction of these bonds and the plane, formed by the X and Y axes. The + and − subscripts denote whether the "upper" end of a bond is in the positive or negative X direction. Lines E and F correspond to the Y_+ and Y_- bonds. These two lines are not well resolved at that orientation but rather the line E appears as a shoulder in the line F.

Let us now look at a given X chain. A part of the chain, consisting of three AsO_4 tetrahedra, linked by two H bonds (one X_+ and one X_-) is shown schematically in Fig. 5(b). There are two possible deuteron sites in each of the two bonds, labeled as A' and B in the left and A and B' in the right bond. The eigenvector of the largest principal value ϕ_{zz} of the EFG tensor points along the direction of the O-D... O bond.[22] The intermediate value ϕ_{yy} lies normal to the plane, formed by the deuteron, its nearest oxygen and the arsenic ion in the middle of the AsO_4 tetrahedron. ϕ_{yy} from the two deuteron sites A and B makes angle ±35° with respect to the Z axis, which makes these two sites physically inequivalent and gives rise to resolved lines in the spectrum. From crystal symmetry it follows that sites A and A' have the same EFG

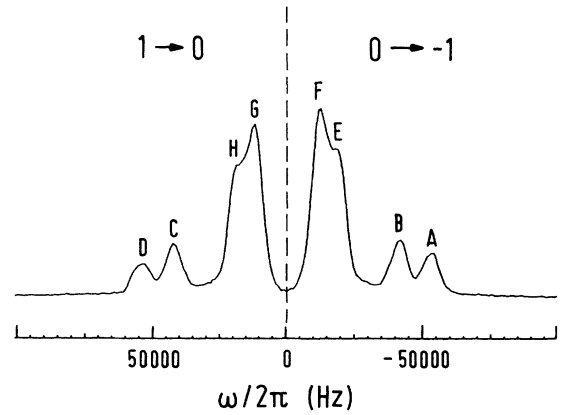

FIG. 4. One-dimensional O-D... O deuteron spectrum of $Rb_{0.68}(ND_4)_{0.32}D_2AsO_4$ at $T=40$ K and orientation $\mathbf{a}\perp\mathbf{H}_0, \angle\mathbf{c},\mathbf{H}_0=45°$ [$\nu_0(^2H)=41.403$ MHz]. For the spectral lines assignation see text.

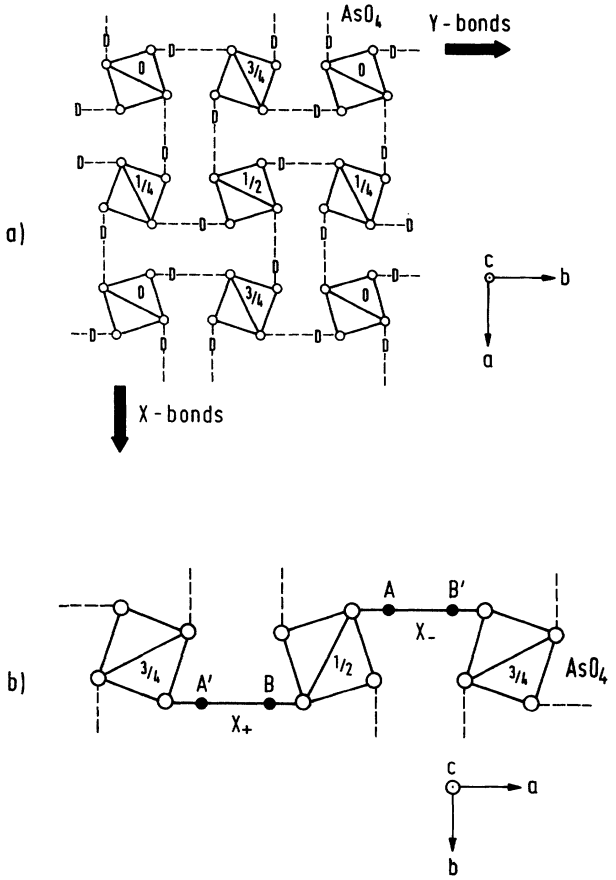

FIG. 5. (a) The projection of the DRADA crystal structure onto the (a,b) plane, showing the H-bond network. (b) A part of the X-bond chain, showing one X_+ and one X_- H bond, linking adjacent AsO_4 tetrahedra. Deuteron sites A and A' are physically equivalent due to the same orientation of the EFG tensor principal axes. The same holds for the sites B and B'. The sites A and B are physically inequivalent and give rise to resolved lines in the spectrum.

tensors and are thus physically equivalent, contributing to the intensity of the same absorption line. The same is true for sites B and B'. At high temperatures fast intrabond motion $A \leftrightarrow B'$ and $A' \leftrightarrow B$ averages the two EFG tensors, resulting in a tensor with ϕ_{yy} in the Z direction and a single line in the spectrum. In a 2D exchange spectrum we expect the intrabond exchange cross peaks to appear between the peaks A and B of Fig. 4 (and the mirror situation on the other two satellites C and D). A similar situation should appear for the $Y_{\pm}$ bonds (lines E and F), but the lines are not well resolved and the cross peaks are less clear to observe. Two-dimensional exchange spectroscopy is a powerful method to detect the intrabond motion in the limit of slow exchange, i.e., when the motion is slow compared to the splitting of the resonance lines of the two exchanging sites. A 2D O-D. . . O deuteron exchange spectrum in DRADA-32 at $T=40$ K is shown in Fig. 6(a) as a contour plot and in Fig. 6(b) as a three-dimensional plot. The mixing time is taken $\tau_m=5$ s. In the evolution period 80 t_1 values were sampled with an increment $\Delta t_1=2$ μs. The signal was zero filled in t_1 to 512 points before Fourier transformation. In the detection period 1 K of complex signal points have been recorded, forming a 512×512 points 2D matrix after a 2D Fourier transformation. Shifted sine-bell windows were used in both domains for the signal apodization. At the end the magnitude spectrum has been computed. Only one repetition of the phase cycle, consisting

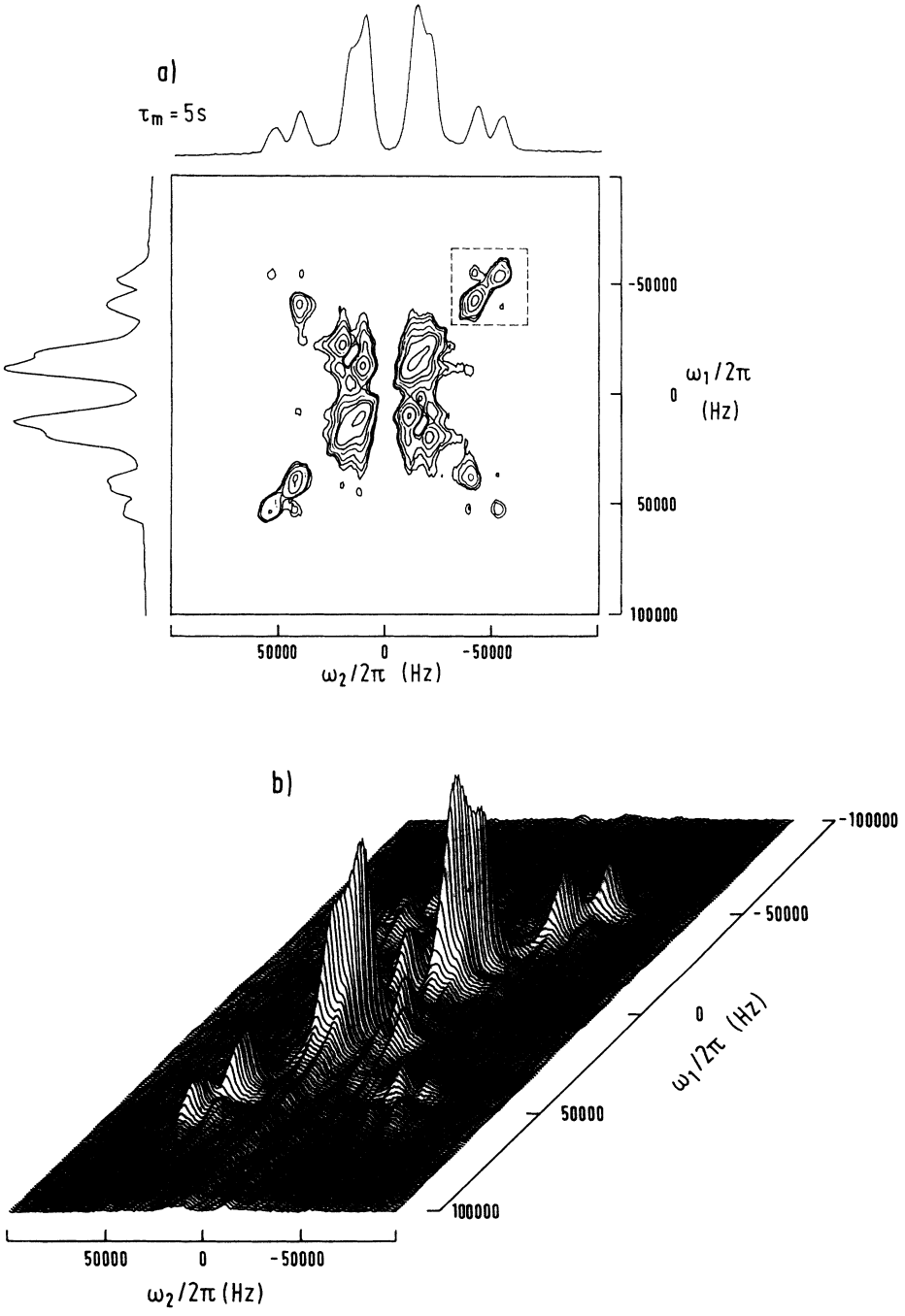

FIG. 6. (a) A 2D O-D. . . O deuteron exchange spectrum in DRADA $x=0.32$ at $T=40$ K, shown as a contour plot. The orientation is the same as that in Fig. 4 and the mixing time is $\tau_m=5$ s. The part of the spectrum, enclosed in a dashed box, corresponds to the $X_{\pm}$ bonds (lines A and B in Fig. 4). (b) Same spectrum displayed as a three-dimensional plot.

of 32 phases (Table I) has been used. At 40 K the pulse sequence was repeated every 150 s, which is about two times the spin-lattice relaxation time, and the whole 2D experiment took 4 days of continuous acquisition. Thus, a good stability of the electronics and temperature control is a necessary prerequisite to perform such experiments. In our case the temperature stability was better than 0.1 K during the whole experiment. In Fig. 6(a), it is seen that there are absorption lines lying on both diagonals of the 2D spectrum. The two diagonals represent two mirror copies of the same spectrum, arising from the fact that the signal is real in t_1 and complex in t_2,

$$S(t_1,t_2)\propto\cos\omega^{(e)}t_1 e^{i\omega^{(d)}t_2} .$$

The fact that the two copies do not have the same intensity is due to the nonunitary character of the mixing propagator.[19] For the analysis of the spectrum only one copy needs to be considered, which we take for convenience from the upper right to the lower left corner of the 2D matrix.

In Fig. 6(a) the two lines A and B are enclosed in a dashed box. The cross peaks are clearly seen and form, with the diagonal peaks, a square. The intensities of the diagonal peaks come from those deuterons, which during the mixing time stayed at their initial positions, located either in the left or right site of the double potential H bond (Fig. 2). The intensities of the two cross peaks arise from the deuterons, which during mixing period jumped either from left to right site or in the opposite direction. The existence of the cross peaks is a direct evidence for the deuteron intrabond exchange and is up to the authors' knowledge the first direct evidence for that.

A systematic study of the exchange motion has been made by varying the mixing time at different temperatures from 45 to 24 K. Part of the spectrum, corresponding to the X bonds [dashed box of Fig. 6(a)] is shown in Fig. 7 at 40 K for three mixing times $\tau_m=1$, 10, and 30 s. The peak assignation is shown as an inset in Fig. 7. The ratio of the cross to diagonal peak intensities $R(\tau_m)=\langle a_{BA}(\tau_m)\rangle/\langle a_{AA}(\tau_m)\rangle$ versus τ_m is shown in Fig. 8(a) for four different temperatures 45, 40, 35, and 24 K. What is remarkable is that at all temperatures the saturated value $R(\infty)=\langle a_{BA}(\infty)\rangle/\langle a_{AA}(\infty)\rangle$ is equal to one and not less than one, as predicted from Eqs. (20a), (20c), and (22) for a static glass. Using the values[13] of q_{EA} for DRADP-44, which is very similar to the DRADA-32, one should get the saturated values as low as $R(\infty)=0.32$ at 50 K, 0.27 at 40 K and 0.13 at 20 K.

The above results are clearly incompatible with the prediction for a static glass. As shown in Eq. (19b) the saturated value $R(\infty)$ equals to unity only when all individual H bonds are symmetric. The curves of Fig. 8(a) have been fitted by Eq. (19a) and the correlation times $\tau_{exch}=\Omega_0^{-1}$ are plotted versus temperature in Fig. 8(b). The slowness of the exchange process is demonstrated by macroscopic values of τ_{exch}. At $T=45$ K, $\tau_{exch}=14.4$ s and at $T=24$ K it amounts to 236 s. τ_{exch} acts as thermally activated, $\tau_{exch}=\tau_0 e^{E_a/kT}$, with $E_a=12.8$ meV and $\tau_0=0.43$ s. This is very different from the single-particle deuteron intrabond jump time $\tau_c=\tau_\infty e^{E_a/kT}$ with $E_a=74$ meV and $\tau_\infty=2.8\times10^{-12}$ s as determined from deuteron spin-lattice (T_1) data.[23] The difference in the attempt frequencies τ_0^{-1} and τ_∞^{-1} is 11 orders of magnitude. The unusually large value of $\tau_0=0.43$ s points to a fact that the 2D exchange experiment does not observe a single-particle motion but a correlated motion of a larger ensemble of particles like clusters of microdomains. This slow motion restores ergodicity of the glassy phase on time scales $t>\tau_{exch}$. The increase of the size of the basic reorientable electric dipole should be however accomplished by an increase of the activation energy, which is not observed in this case. The τ_0 and E_a values have been determined from the assumption of an Arrhenius type of thermally activated motion which does not reproduce

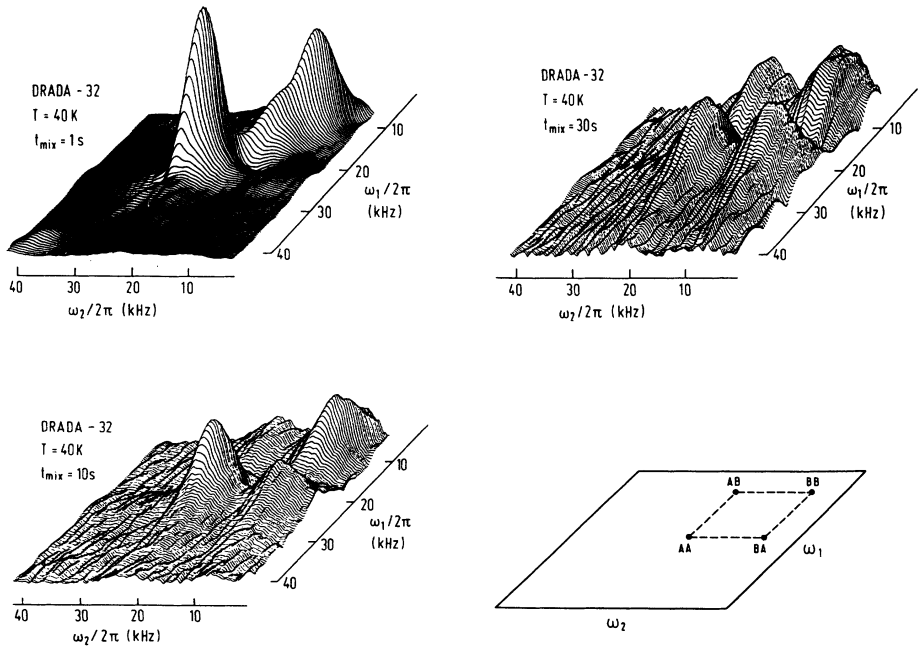

FIG. 7. O-D...O deuteron 2D exchange spectrum in DRADA $x=0.32$ at $T=40$ K for three different mixing times $\tau_m=1$, 10, and 30 s. Only the part of the spectrum corresponding to the X bonds [dashed box of Fig. 6(a)] is shown. At long mixing times cross peaks and diagonal peaks have the same intensities. In the lower right corner the assignation of the peaks in the 2D spectrum is shown.

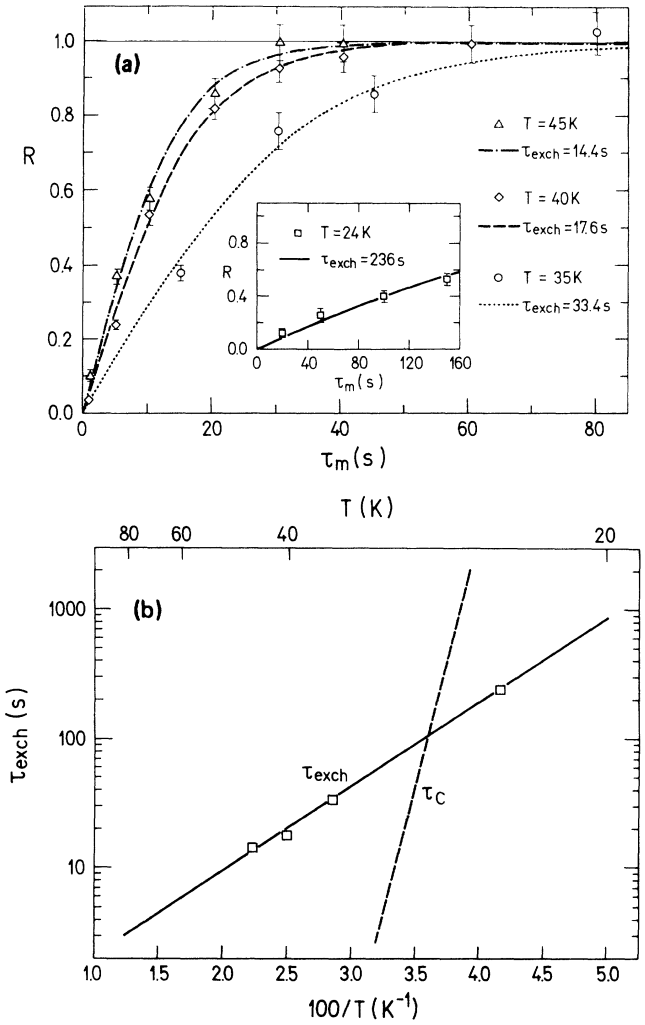

FIG. 8. (a) Experimental ratio of the cross peak to diagonal peak intensities $R(\tau_m)$ vs the mixing time τ_m at four different temperatures $T=45$, 40, 35, and 24 K. The curves represent the fit with Eq. (19a), describing the case when all H bonds are symmetric. (b) Temperature dependence of the intra-H-bond deuteron exchange time $\tau_{\text{exch}}=\Omega_0^{-1}$, determined from 2D NMR. The single-particle intra-H-bond jump time τ_c, extrapolated from the T_1 minimum around 90 K, is shown as a dashed line.

correctly also the low-temperature T_1 data[14] in DRADP $x=0.44$. A more elaborate model of the O-D. . . O intrabond motion, taking into account tunneling, seems to be necessary to clarify this point.

The same behavior of the cross and diagonal peak intensities ratio can be predicted also from a spin-diffusion effect. The spin-diffusion time constant is, however, temperature independent[24] which is to be contrasted with the thermally activated form of τ_{exch} in Fig. 8(b). Another test to prove or eliminate the presence of spin diffusion is to vary the frequency separation between X_+ and X_- deuteron lines, which can be achieved by changing the orientation of the crystal in the magnetic field. The spin-diffusion time constant in the weakest case increases as the square of the frequency distance between the lines,[24] $T_{\text{SD}} \propto (\Delta\nu)^2$. Stronger dependencies like[24] $T_{\text{SD}} \propto (\Delta\nu)^4$ and exponential[25] have also been predicted. We performed two sets of 2D exchange experiments at $T=40$ K for two different orientations and plot the $R(x)$ curves. The first experiment has been made at the orientation $\mathbf{a}\perp\mathbf{H}_0, \angle\mathbf{c},\mathbf{H}_0=45°$, where the $X_\pm$ splitting amounts to 11.3 kHz whereas the second has been made at the orientation $\mathbf{a}\perp\mathbf{H}_0, \angle\mathbf{c},\mathbf{H}_0=65°$ with $X_\pm$ splitting of 8.7 kHz. At these two orientations $X_\pm$ and $Y_\pm$ do not overlap. The $X_\pm$ splitting at $\angle\mathbf{c},\mathbf{H}_0=45°$ is 30% larger than the one at $\angle\mathbf{c},\mathbf{H}_0=65°$, which should yield in the weakest case [$T_{\text{SD}} \propto (\Delta\nu)^2$] about 70% larger time constant. No change in the exchange time has however been detected (Fig. 9), which together with the thermally activated form of τ_{exch} rules out the effects of spin diffusion.

VI. O-D. . . O DEUTERON INTERBOND ($X \leftrightarrow Y$) EXCHANGE IN $Rb_{0.68}(ND_4)_{0.32}D_2AsO_4$

In addition to the intra-H-bond exchange, O-D. . . O deuterons also undergo exchange between different X and Y bonds. This interbond exchange has been first studied by Schmidt and Uehling[19] in DKDP. They selectively saturated X-bond deuteron quadrupole perturbed Zeeman NMR line. This saturation was in the course of time transferred into the Y-bond line by the deuteron $X \leftrightarrow Y$ exchange. The average correlation time for the XY ex-

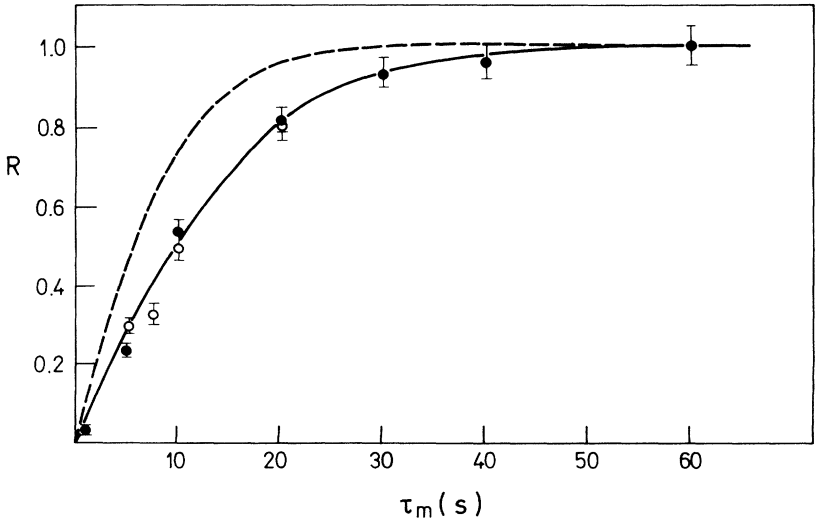

FIG. 9. Experimental ratio of the deuteron cross to diagonal peak intensities $R(\tau_m)$ vs the mixing time τ_m at $T=40$ K in DRADA $x=0.32$. Two experiments have been performed at two different orientations: (a) $\mathbf{a}\perp\mathbf{H}_0, \angle\mathbf{c},\mathbf{H}_0=45°$ (solid circles) where the $X_\pm$ deuteron lines splitting amounts to 11.3 kHz; (b) $\mathbf{a}\perp\mathbf{H}_0, \angle\mathbf{c},\mathbf{H}_0=65°$ (open circles) with $X_\pm$ splitting of 8.7 kHz. Solid line represents the fit $R(\tau_m)=\tanh(\tau_m/\tau_{\text{exch}})$ with $\tau_{\text{exch}}=14.4$ s. Dashed line represents a calculated curve $R(\tau_m)=\tanh(\tau_m/T_{\text{SD}})$, which would be obtained at the orientation with 8.7-kHz splitting in case of spin diffusion, assuming quadratic dependence of T_{SD} on the line separation [$T_{\text{SD}} \propto (\Delta\nu)^2$].

change at room temperature was found to be $\tau_{XY} \approx 0.4$ s. The exchange was thermally activated with the activation energy $E_a = 0.58$ eV. Extrapolated to temperatures below $T_G \approx 90$ K, where the glassy phase in DRADP and DRADA exists, this gives unphysically large exchange times τ_{XY} and the interbond motion is effectively frozen on the experimental time scale. The interbond motion does not participate in the formation of the glassy phase and only the intrabond motion has to be considered in this context. It is, however, interesting to observe directly the deuteron inter-XY-bond exchange with the 2D exchange NMR at temperatures high enough that τ_{XY} is reasonably short, e.g., at room temperature. In the case of interbond exchange one expects cross peaks between the X and Y deuteron lines in the 2D spectrum. The existence of the cross peaks gives a direct evidence for the

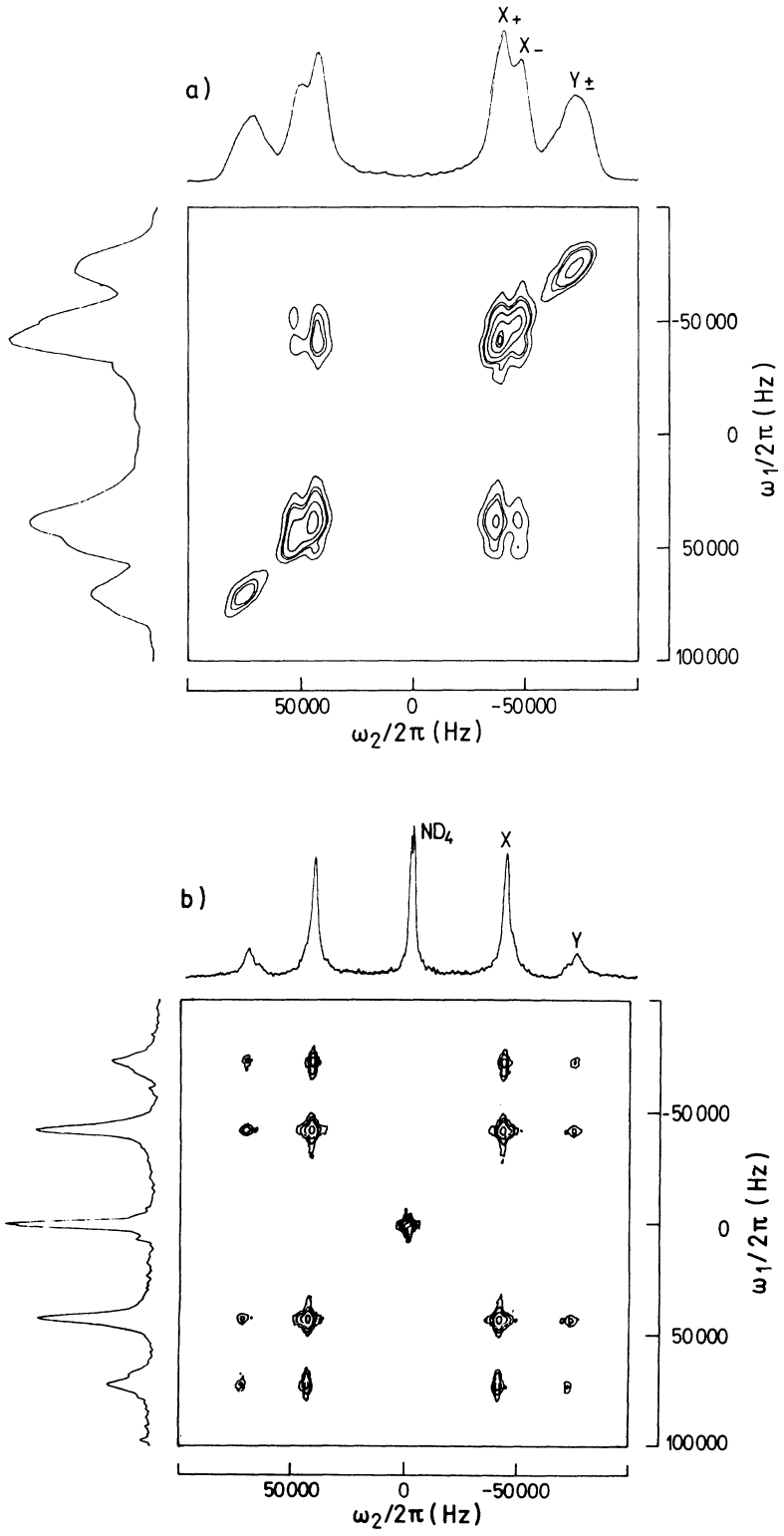

FIG. 10. (a) A 2D O-D...O deuteron exchange spectrum in DRADA $x = 0.32$ at $T = 40$ K and an orientation $\mathbf{a} \perp \mathbf{H}_0, \angle \mathbf{c}, \mathbf{H}_0 = 65°$ [$\nu_0(^2\mathrm{H}) = 41.463$ MHz]. The mixing time is $\tau_m = 5$ s. $X_\pm$ deuteron lines are partially resolved, whereas $Y_\pm$ lines overlap, as can be seen from the 1D spectrum at the top. The intrabond exchange is manifested in the square-like shape of the contour plots of the X-bond lines. The absence of the cross peaks between X and Y lines indicates the absence of interbond (XY) exchange at this temperature. (b) The same experiment repeated at $T = 293$ K using the mixing time $\tau_m = 0.4$ s. $X_\pm$ and $Y_\pm$ splittings are averaged out by the fast O-D...O deuteron intrabond motion, yielding sharp X and Y lines. In the middle of the spectrum the rotationally averaged ND_4 deuteron line is observed. The cross peaks between the X and Y lines now appear, giving a direct proof for the existence of the interbond (XY) exchange at room temperature.

XY exchange.

The 2D deuteron exchange experiment has been performed in $Rb_{0.68}(ND_4)_{0.32}D_2AsO_4$ at an orientation $\mathbf{a}\perp\mathbf{H}_0, \angle\mathbf{c},\mathbf{H}_0=65°$ at two temperatures $T=40$ and 293 K. At this orientation the inner pair of lines corresponds to the X-bond O-D. . . O deuterons and the outer pair to the Y-bond deuterons. The 2D exchange spectrum at $T=40$ K is displayed in Fig. 10(a) for the mixing time $\tau_m=5$ s. The corresponding 1D spectrum [projection at the top of Fig. 10(a)] shows partially resolved X_+ and X_- lines, whereas $Y_\pm$ lines overlap and give one broad line. The intrabond exchange at this temperature is manifested in the squarelike shape of the contour plots of the X-bond lines, since the peaks are not resolved enough to give resolved diagonal and cross peaks. There are, however, no cross peaks between X and Y lines, indicating the absence of interbond (XY) exchange at this temperature. The experiment has been repeated at $T=293$ K using the mixing time $\tau_m=0.4$ s under otherwise identical conditions [Fig. 10(b)]. At this temperature $X_\pm$ and $Y_\pm$ splittings are no more observed as they are averaged out by the fast deuteron intrabond motion. The 1D spectrum displays sharp X and Y O-D. . . O lines and an additional ND_4 deuteron line in the middle of the spectrum. The ND_4 line cannot be observed at low temperatures, since after the ND_4 rotation freeze-out below $T\approx 100$ K this line disappears from the spectrum. What is remarkable in the 2D spectrum is the appearance of the cross peaks between the X and Y lines, giving a direct proof for the existence of the interbond (XY) exchange at room temperature. No systematic variation of τ_m has been made in our measurements and we did not determine the interbond exchange time τ_{XY}. The appearance of the cross peaks for $\tau_m=0.4$ s is, however, in agreement with the expectations from the DKDP (Ref. 19) results where $\tau_{XY}=0.4$ s at room temperatures has been determined.

VII. DISCUSSION

It is now clear why the NMR line-shape and spin-lattice relaxation studies see the glassy disorder as static. These techniques are sensitive to the molecular motions in the 10^8-10^3 Hz window. A motion with milli-Hz frequencies appears static on this time scale. When observed with a technique, sensitive to motions in an observation window at lower frequencies, the glass disorder turns out to be a dynamic phenomenon. This suggests the answer to the question whether in the case of proton glasses we deal with a new kind of a thermodynamic phase transition, or the appearance of a glass state is a kinetic phenomenon. By observing the system on a short time scale, there is a lot of evidence for an equilibrium ergodic-nonergodic phase transition and the random-bond–random-field theory[9] correctly describes the features of the glass phase. In this theory the local polarization of a given H bond is given by

$$p_i=\langle S_i^z\rangle \ , \tag{25}$$

where S_i^z represents the Ising pseudospin,[26] $S_i^z=\pm 1$ and the brackets $\langle\cdots\rangle$ represent a thermodynamic (mean-field) average. The average polarization of all bonds in the glass phase vanishes,

$$\bar{p}=\frac{1}{N}\sum_i \langle S_i^z\rangle=[\langle S_i^z\rangle]_{\rm av}=0 \ . \tag{26}$$

Here the summation goes over all H bonds, N is the number of lattice sites, and $[\cdots]_{\rm av}$ denotes the disorder average,[8] i.e., the simultaneous average over random bonds and random fields. The average square local polarization is however different from zero as the bonds are polarized but in a random spatial manner. The free energy of a glassy state in a phase space is believed to be highly degenerate exhibiting many global and local minima [Fig. 11(a)]. The pseudospin system can in general visit many of these minima and the order parameter appropriate to describe such a case is the "multivalley" order parameter[6]

$$q=\frac{1}{N}\sum_i\left[\sum_l P_l\langle S_i^z\rangle_l\right]^2 =\left[\left[\sum_l P_l\langle S_i^z\rangle_l\right]^2\right]_{\rm av} \ . \tag{27}$$

Here P_l is the probability of finding the system in the lth valley and the summation over all valleys is made. An experiment over a short time however measures the properties of the system effectively locked in one of the global or local minima. Such "single-valley" order parameter corresponds to the case of infinitely high barriers ΔU between different valleys. This order parameter is of the

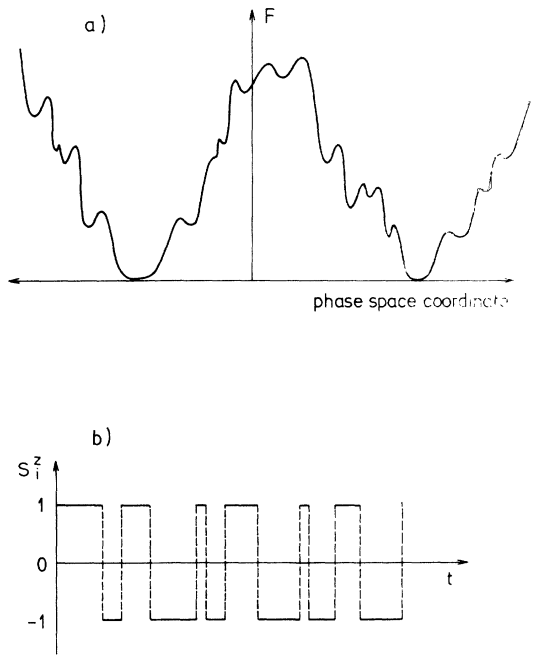

FIG. 11. (a) Free-energy surface in phase space of a glassy state exhibiting degeneracy with many global and side minima. (b) Time dependence of the pseudospin variable S_i^z, reflecting random jumps of proton or deuteron between two possible sites in the H bond.

"Edwards-Anderson" type

$$q_{\mathrm{EA}}=\frac{1}{N}\sum_i \langle S_i^z\rangle^2=[\langle S_i^z\rangle^2]_{\mathrm{av}} \tag{28}$$

and is obtained from the multivalley order parameter q when all the probabilities P_l are equal to zero, except one which is equal to 1.

The above definitions of p_i, q, and q_{EA} are made on the basis of a static model. It is possible, however, to define these quantities also in terms of dynamics. The S_i^z variable assumes in time randomly the values ± 1 [Fig. 11(b)]. The time-dependent local polarization is obtained as the time integral of $S_i^z(t)$ over the observation time t_{obs}:

$$p_i(t_{\mathrm{obs}})=\frac{1}{t_{\mathrm{obs}}}\int_0^{t_{\mathrm{obs}}} S_i^z(t)dt \ . \tag{29}$$

In the limit $t_{\mathrm{obs}}\to\infty$ one obtains the equilibrium polarization p_i [Eq. (25)]. The time-dependent glass order parameter is obtained as an average time-autocorrelation function[6] of S_i^z:

$$q(t)=[\langle S_i^z(0)S_i^z(t)\rangle_{t'}]_{\mathrm{av}} \ , \tag{30}$$

where the time average $\langle\cdots\rangle_{t'}$ is performed over an observation time t_{obs}:

$$\langle S_i^z(0)S_i^z(t)\rangle_{t'}=\frac{1}{t_{\mathrm{obs}}}\int_0^{t_{\mathrm{obs}}} dt'[S_i^z(t')S_i^z(t'+t)] \ . \tag{31}$$

Edwards-Anderson (single-valley) order parameter q_{EA} is obtained as the limiting case of $q(t)$ when the barriers between the valleys ΔU diverge and the time t tends to infinity

$$q_{\mathrm{EA}}=\lim_{t\to\infty}\lim_{\Delta U\to\infty} q(t) \ . \tag{32}$$

If the barriers stay finite we obtain the multivalley order parameter q

$$q=\lim_{t\to\infty} q(t) \ . \tag{33}$$

Another interesting limit is obtained with regard to t_{obs}. In the limit of an infinitely short observation time one observes an "instant-time" picture, where the system is in a single valley and everything is perfectly ordered in the moment of observation, yielding

$$\lim_{t_{\mathrm{obs}}\to 0} q(t)=1 \ . \tag{34}$$

In the intermediate case when t_{obs} in neither infinitely short nor infinitely long the value of $q(t)$ actually depends on the integration time t_{obs} and will thus depend on the observation window in frequency space of different experimental techniques. What is important is the relation between the frequency windows of experimental measurement techniques and internal molecular motions. Observation of the system with a window much higher in frequency than the frequencies of molecular motions will probe the system as completely frozen static, whereas the dynamic character appears in observation with the frequency window shifted towards lower frequencies.

In deuteron glasses the glassy phase appears as a consequence of the deuteron intra-H-bond motion freeze-out. In a NMR spin-lattice and line-shape experiment below 70 K we observe the system on the time scale much shorter than the characteristic deuteron intrabond exchange time τ_{exch} and the ergodicity is broken. The glass phase appears ordered and the order parameter is different from zero. In a 2D NMR exchange experiment the observation time becomes long compared to τ_{exch}. The slow intrabond exchange restores ergodicity, the time correlation of S_i^z [Eq. (30)] is lost and $q(t)$ tends towards zero.

The glass order parameter thus depends on the observation time—or frequency—window of the applied experimental technique. Similar time-dependent effects in a glass state of a polymer have been reported[27] by the use of multidimensional NMR. There the authors analyzed the nonexponential behavior of the relaxation processes in the glass state. They found the distribution of correlation times to be heterogeneous (nonergodic) on the time scale of the average correlation time, becoming homogeneous (ergodic) at later times due to fluctuations which were 2 orders of magnitude slower. This time-recovered homogeneous distribution shows a Markovian character of the system where the ergodicity is inherent in the Markovian type of motion.

The fact that the experimental $R(\tau_m\to\infty)$ curves of Fig. 8 all reach the value 1, yielding zero glass order parameter, can be explained as follows. This results cannot be obtained for the model of a static glass, since all the bond asymmetries Δ should be strictly zero during the time of the experiment. This is a completely unphysical assumption for the proton glasses. The results can be, however, explained by considering the asymmetries to be time dependent, $\Delta=\Delta(t)$, as a consequence of the thermal motion of the lattice. In a 2D exchange experiment one observes the time average asymmetry $\overline{\Delta(t)}$, where the average is made over the observation time. Since all other time intervals in the pulse sequence of Fig. 1 are of negligible duration compared to the mixing time τ_m, one can attribute the time dependence of Δ solely to τ_m, $\overline{\Delta(t)}=\overline{\Delta(\tau_m)}$. The time average asymmetry can be much smaller than the instant value of $\Delta(\tau_m)$ and eventually becomes zero, yielding zero value of the glass order parameter as determined from the $R(\tau_m\to\infty)$ curves. To consider the glassy phase for long observation times a dynamic glass theory is needed. Such theory has not been made so far.

VIII. CONCLUSIONS

Two-dimensional exchange NMR results show that the glass state in proton glasses is not a thermodynamic long-lived state but rather a dynamic phenomenon. It shows a frozen-in static disorder only when observed with observation windows in the frequency range which is smaller than the full width of the spectrum of correlation times for internal motions. In the limit of long observation times, the asymmetries of the H-bonds—which play the essential role in the formation of the glass phase in proton or deuteron glasses—show a time-averaged symmetric form, leading to no net time-average order of deuterons in H bonds. The static random-bond–random-field (PTB) (Ref. 9) pseudospin Ising model provides for a valid description of deuteron glasses for observation times short compared to the O-D... O intra-

bond exchange time, which at $T=30$ K amounts to several hundred seconds. For longer observation times a dynamic theory is necessary. Unfortunately it does not exist as yet.

The observed ergodicity breaking in deuteron glasses on short-time scales and ergodicity recovering on long-time scales may provide for a conceptual link between the glass transition and classical structural transitions. In glasses the free-energy hypersurface in the N-dimensional phase space of local polarizations is rough, microdomains are small and ergodicity is restored on long enough time scales, whereas in the case of ferroelectric and other structural transitions the free-energy surface is smooth, the domains are macroscopic, and the lifetime for spontaneous domain reorientation is essentially infinite.

APPENDIX A: 2D EXCHANGE SPECTRUM IN THE PRESENCE OF TWO DIFFERENT RELAXATION RATES

Here we analyze the effect of spin-lattice relaxation on the cross to diagonal peak ratio $R(x)$ in the case that nuclei experience different relaxation rates in the two sites A and B of the H bond. We are interested to see how different relaxation rates affect the saturated value of the cross to diagonal peak ratio $R(\infty)$ in the glassy state using the random-bond–random-field model. In case of a single relaxation rate this model predicts $R(\infty)$ to be always less than unity except in the trivial case when all the bond asymmetries are zero and $R(\infty)=1$. The microscopic reason why the relaxation rates $r_A=1/T_{1A}$ and $r_B=1/T_{1B}$ of the two sites differ need not be specified explicitly for the purpose of this calculation. One obvious reason could be the fact that the two EFG tensors of the sites A and B differ. The lattice vibrations could thus produce different quadrupolar relaxation at the two sites in the absence of nuclear exchange. In the presence of fast nuclear exchange the two relaxation rates will be replaced by a single effective one as known from the theory of exchange processes.

We use the same formalism[18] as before and compute the diagonal and cross peak intensities which replace Eqs. (11a)–(11c) in the case $r_A \neq r_B$. We get

$$a_{AA}(\tau_m)=\frac{1}{4\varepsilon'\cosh(\Delta/2kT)}e^{\Delta/2kT}e^{-\tau_m[\Omega_0\cosh(\Delta/2kT)+(r_A+r_B)/2]}\{(\varepsilon'+\kappa')e^{-\varepsilon'\tau_m}+(\varepsilon'-\kappa')e^{\varepsilon'\tau_m}\}\ , \tag{A1}$$

$$a_{BB}(\tau_m)=\frac{1}{4\varepsilon'\cosh(\Delta/2kT)}e^{-\Delta/2kT}e^{-\tau_m[\Omega_0\cosh(\Delta/2kT)+(r_A+r_B)/2]}\{(\varepsilon'-\kappa')e^{-\varepsilon'\tau_m}+(\varepsilon'+\kappa')e^{\varepsilon'\tau_m}\}\ , \tag{A2}$$

$$a_{AB}(\tau_m)=a_{BA}(\tau_m)=\frac{1}{4\varepsilon'\cosh(\Delta/2kT)}e^{-\tau_m[\Omega_0\cosh(\Delta/2kT)+(r_A+r_B)/2]}\Omega_0(e^{\varepsilon'\tau_m}-e^{-\varepsilon'\tau_m})\ . \tag{A3}$$

κ' and ε' are defined as

$$\kappa'=\frac{r_A-r_B}{2}-\Omega_0\sinh\frac{\Delta}{2kT}\ , \tag{A4}$$

$$\varepsilon'=\sqrt{\kappa'^2+\Omega_0^2}\ . \tag{A5}$$

We now apply these results to the glassy state. We average Eqs. (A1)–(A3) over the distribution function $\rho(\Delta)$ of bond asymmetries. Let us first recall the case $r_A=r_B$. There we find from Eq. (18a) that the diagonal peaks have the same intensities $\langle a_{AA}(x)\rangle=\langle a_{BB}(x)\rangle$ as a consequence of the fact that $\rho(\Delta)=\rho(-\Delta)$ is symmetric and we are integrating on a symmetric interval. The cross peaks also have the same intensities $\langle a_{AB}(x)\rangle=\langle a_{BA}(x)\rangle$, as seen from Eq. (17c). We thus have for the case $r_A=r_B$ a single cross to diagonal peak intensity ratio $R(x)$ which is the same for both pairs of cross and diagonal peaks,

$$R(x)=\frac{\langle a_{BA}(x)\rangle}{\langle a_{AA}(x)\rangle}=\frac{\langle a_{AB}(x)\rangle}{\langle a_{BB}(x)\rangle}\ . \tag{A6}$$

The situation is different in the case $r_A\neq r_B$. Let us define $r_B=\lambda r_A$, $r_A=\mu\Omega_0$, and introduce parameter

$$\gamma=\frac{r_A-r_B}{2\Omega_0}=\frac{\mu(1-\lambda)}{2}\ .$$

We take r_A to be smaller of the two relaxation rates ($\lambda\geq 1$) and larger than Ω_0 ($\mu>1$). γ falls in the interval $[-\infty,0]$ and $\gamma=0$ represents the $r_A=r_B$ case. We define the quantities

$$R_1(x)=\frac{\langle a_{BA}(x)\rangle}{\langle a_{AA}(x)\rangle}\ , \tag{A7a}$$

$$R_2(x)=\frac{\langle a_{AB}(x)\rangle}{\langle a_{BB}(x)\rangle}\ , \tag{A7b}$$

which represent the cross to diagonal peak intensity ratios of two distinct pairs of cross and diagonal peaks. $R_1(x)$ and $R_2(x)$ have been calculated numerically (Fig. 12) for a number of γ values using Eqs. (A1)–(A5). Inspecting the limiting behavior of $R_1(x)$ and $R_2(x)$ for $x\to\infty$ we find that the two ratios $R_1(\infty)$ and $R_2(\infty)$ are no more equal as in the $\gamma=0$ case. The cross peaks still have the same intensities, but the diagonal peaks now differ. Consequently R_1 falls below the value of R obtained in the $r_A=r_B$ ($\gamma=0$) case, whereas R_2 lies above R. The random-bond–random-field distribution function of bond asymmetries $g(u)$ [Eq. (24d)] has been used which is related to $\rho(\Delta)$ [Eqs. (16b) and (16c)]. The curves are calculated for $T=50$ K and glass parameters $T_G=90$ K and $\bar{\Delta}=0.35$. Using these parameters we obtain in the case $r_A=r_B$ ($\gamma=0$) a saturated value of the cross to diagonal peak intensity ratio $R(\infty)=0.26$. $R_1(x)$ always lies below this value and continuously approaches zero for $x\to\infty$ whereas $R_2(x)$ lies above for all $\gamma<0$ values and continuously grows towards infinity for

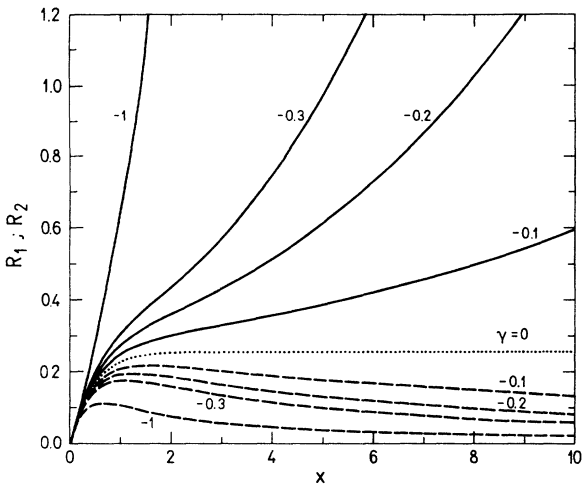

FIG. 12. The calculated ratios of the cross to diagonal peak intensities $R_1(x)=\langle a_{BA}(x)\rangle/\langle a_{AA}(x)\rangle$ (dashed lines) and $R_2(x)=\langle a_{AB}(x)\rangle/\langle a_{BB}(x)\rangle$ (solid lines) as a function of the normalized mixing time $x=\Omega_0\tau_m$ in the case that the spin-lattice relaxation rates r_A and r_B of the two sites A and B in the H-bond double-potential differ. The calculation has been made for a static glass (random-bond–random-field model) at $T=50$ K using model parameters $T_G=90$ K and $\bar{\Delta}=0.35$. Parameter $\gamma=\mu(1-\lambda)/2$ has been varied between 0 and -1 ($r_B=\lambda r_A$, $r_A=\mu\Omega_0$) and $\gamma=0$ curve (dotted line) represents the case $r_A=r_B$, corresponding to the curves of Fig. 13.

$x\rightarrow\infty$. For long mixing times neither of the two ratios R_1 and R_2 reaches a constant plateau as in the $r_A=r_B$ case and the difference R_2-R_1 is growing continuously.

The main feature emerging from the difference of the spin-lattice relaxation rates r_A and r_B is the fact that one has to distinguish between two kinds of cross to diagonal peak intensity ratios, belonging to two pairs of cross and diagonal peaks. Each pair is affected by the spin-lattice relaxation in the opposite sense. In the limit $x\rightarrow\infty$ one of them tends towards zero and the other grows continuously to a value which can be much larger than unity. These results cannot give an alternative explanation to our "ergodicity restoring" results where for long mixing times in DRADA we obtain all cross and diagonal peak intensities to be the same (see spectrum with $\tau_m=30$ s in Fig. 7) and both ratios $R_1(\infty)$ and $R_2(\infty)$ are equal to one.

APPENDIX B: 2D EXCHANGE SPECTRUM IN THE PRESENCE OF A DISTRIBUTION OF RELAXATION RATES

In this appendix we analyze the influence of spin-lattice relaxation on the cross to diagonal peak intensity ratio for the case that T_1 depends on the asymmetry Δ of the bond, $T_1=T_1(\Delta)$. Since in the glassy state asymmetries Δ are distributed with the distribution function $\rho(\Delta)$ we are dealing also with a distribution of relaxation rates $[T_1(\Delta)]^{-1}$.

The quadrupolar spin-lattice relaxation rate for the spin $I=1$ case can be written as

$$\frac{1}{T_1}=W_1+2W_2\ . \tag{B1}$$

Here W_1 and W_2 represent the $\Delta m=\pm1$ and $\Delta m=\pm2$ transition probabilities, which depend on the time fluctuating parts of the EFG tensor elements $\Delta V_{ij}(t)$:

$$W_1=4\left[\frac{E}{\hbar}\right]^2\int_{-\infty}^{\infty}[\overline{\Delta V_{zy}(0)\Delta V_{zy}(\tau)}+\overline{\Delta V_{zx}(0)\Delta V_{zx}(\tau)}]e^{i\omega_0\tau}d\tau\ , \tag{B2a}$$

$$W_2=4\left[\frac{E}{\hbar}\right]^2\int_{-\infty}^{\infty}\{\frac{1}{4}[\overline{\Delta V_{xx}(0)\Delta V_{xx}(\tau)}+\overline{\Delta V_{yy}(0)\Delta V_{yy}(\tau)}]+\overline{\Delta V_{xy}(0)\Delta V_{xy}(\tau)}\}e^{2i\omega_0\tau}d\tau\ . \tag{B2b}$$

Here $E=e^2Q/4$, the bar represents an ensemble average, and $\hbar\omega_0$ is the energy difference between two adjacent quadrupole perturbed Zeeman levels.

To evaluate W_1 and W_2 for DRADA we have to look at the EFG tensor of deuterons. In the crystal fixed frame the tensor has the following form:[28]

$$\underline{V}=\begin{bmatrix} V_{aa} & 0 & \pm V_{ac} \\ 0 & V_{bb} & \pm V_{bc} \\ \pm V_{ac} & \pm V_{bc} & V_{cc} \end{bmatrix}\ . \tag{B3}$$

The elements V_{ac} and V_{bc} fluctuate between $\pm$ values due to the intrabond exchange of deuterons and only these two have to be considered as time dependent in this calculation. We transform the tensor into the laboratory frame and compute time-dependent elements for the orientation $\mathbf{a}\perp\mathbf{H}_0,\angle\mathbf{c},\mathbf{H}_0=45°$, where the measurements have been made. We find four time-dependent elements:

$$V_{yy}(t)=-V_{bc}(t)\ ,$$
$$V_{zz}(t)=V_{bc}(t)\ ,$$
$$V_{xy}(t)=-\sqrt{2}/2V_{ac}(t)\ ,$$
$$V_{xz}(t)=\sqrt{2}/2V_{ac}(t)\ .$$

We write the elements $V_{ac}(t)$ and $V_{bc}(t)$ for a deuteron in a given hydrogen bond in the form

$$V_{ac}(t)=\alpha p(t)\ ,$$
$$V_{bc}(t)=\beta p(t)\ ,$$

where $p(t)$ represents the polarization of the bond. $p(t)$ can be separated into a static part $p=\tanh(\Delta/2kT)$ and a time fluctuating part $\Delta p(t)$:

$$p(t)=p+\Delta p(t)\ .$$

W_1 and W_2 can now be written as

$$W_1=2\alpha^2\left[\frac{E}{\hbar}\right]^2\int_{-\infty}^{\infty}\overline{\Delta p(0)\Delta p(\tau)}e^{i\omega_0\tau}d\tau\ , \tag{B4a}$$

$$W_2=2\alpha^2\left[\frac{E}{\hbar}\right]^2\left[1+\frac{\beta^2}{2\alpha^2}\right]\int_{-\infty}^{\infty}\overline{\Delta p(0)\Delta p(\tau)}e^{2i\omega_0\tau}d\tau\ . \tag{B4b}$$

The autocorrelation function $\overline{\Delta p(0)\Delta p(\tau)}$ can be written as[16]

$$\overline{\Delta p(0)\Delta p(\tau)}=(1-p^2)e^{-\tau/\tau_c} \tag{B5}$$

and the correlation time τ_c is given by

$$\frac{1}{\tau_c}=K_{AB}+K_{BA}=2\Omega_0\cosh\frac{\Delta}{2kT}\ . \tag{B6}$$

We also use $u=\Delta/2kT$ and write $T_1(u)$ using Eqs. (B1), (B4a), and (B4b):

$$\frac{1}{T_1(u)}=\frac{\alpha^2e^4Q^2}{16\hbar^2}\frac{1}{\Omega_0\cosh u}\times\left[\frac{1}{\cosh^2u+\omega_0^2/4\Omega_0^2}+\frac{2+\beta^2/\alpha^2}{\cosh^2u+\omega_0^2/\Omega_0^2}\right]\ . \tag{B7}$$

T_1 is a symmetric function of bond asymmetries, $T_1(u)=T_1(-u)$.

Now we compute the cross and diagonal peak intensities. Equations (11a)–(11c) have to be modified to

$$a_{AA}(\tau_m)=\frac{1}{[2\cosh(\Delta/2kT)]^2}e^{-\tau_m/T_1(\Delta/2kT)}\left[e^{\Delta/kT}+e^{-2\Omega_0\tau_m\cosh(\Delta/2kT)}\right]\ , \tag{B8a}$$

$$a_{BB}(\tau_m)=\frac{1}{[2\cosh(\Delta/2kT)]^2}e^{-\tau_m/T_1(\Delta/2kT)}\left[e^{-\Delta/kT}+e^{-2\Omega_0\tau_m\cosh(\Delta/2kT)}\right]\ , \tag{B8b}$$

$$a_{AB}(\tau_m)=a_{BA}(\tau_m)=\frac{1}{[2\cosh(\Delta/2kT)]^2}e^{-\tau_m/T_1(\Delta/2kT)}\left[1-e^{-2\Omega_0\tau_m\cosh(\Delta/2kT)}\right]\ . \tag{B8c}$$

In the glassy state we have to average these expressions over the symmetric distribution function $\rho(\Delta)$. We transform again to the variable u using Eqs. (16a)–(16c). We define

$$I_a'(x)=\int_{-u_{\max}}^{u_{\max}}du\,g(u)e^{-x/\Omega_0T_1(u)}\frac{e^{2u}}{\cosh^2u}\ , \tag{B9a}$$

$$I_b'(x)=\int_{-u_{\max}}^{u_{\max}}du\,g(u)e^{-x/\Omega_0T_1(u)}\frac{e^{-2x\cosh u}}{\cosh^2u}\ , \tag{B9b}$$

$$I_c'(x)=\int_{-u_{\max}}^{u_{\max}}du\,g(u)e^{-x/\Omega_0T_1(u)}\frac{1}{\cosh^2u}\ . \tag{B9c}$$

The cross to diagonal peak intensity ratio is given by

$$R(x)=\frac{\langle a_{BA}(x)\rangle}{\langle a_{AA}(x)\rangle}=\frac{I_c'(x)-I_b'(x)}{I_a'(x)+I_b'(x)}\ . \tag{B10}$$

Since $g(u)$ and $T_1(u)$ are symmetric and we are integrating on a symmetric interval, we find that the diagonal peaks have the same intensities $\langle a_{AA}(x)\rangle=\langle a_{BB}(x)\rangle$. The ratio $R(x)$ is thus the same for both pairs of cross and diagonal peaks,

$$R(x)=\frac{\langle a_{BA}(x)\rangle}{\langle a_{AA}(x)\rangle}=\frac{\langle a_{AB}(x)\rangle}{\langle a_{BB}(x)\rangle}\ .$$

The ratio $R(x)$ has been calculated numerically, using the random-bond–random-field distribution function $g(u)$ [Eq. (24d)] with the glass parameters $T_G=90$ K and $\tilde{\Delta}=0.35$. The curves are calculated for $T=30$ K and are displayed in Fig. 13. In the calculation we used different $T_1(u=0)$ values as parameters and took $\Omega_0^{-1}=4$ s. This enabled us to evaluate $T_1(u)$ [Eq. (B7)]. Different curves correspond to different $T_1(u=0)$ values, ranging from few seconds to infinity. A comparison to the case of a single constant T_1 [Eq. (18e) and Fig. 3], which is obtained in the limit $T_1(u=0)\to\infty$, is made. From Fig. 13 it is seen that $R(x)$ in case of a distribution of relaxation rates becomes even smaller than in the case of a single constant rate. The reason is the fact that $T_1(u)$ from Eq. (B7) becomes longer for bonds with a larger asymmetry $u=\Delta/2kT$. The diagonal and cross peak intensities are T_1 weighted sums of the contributions from all individual

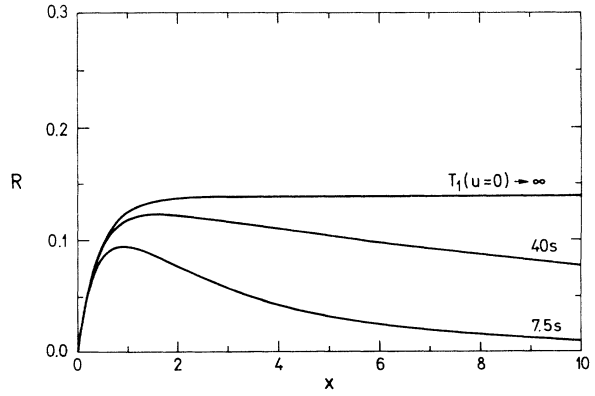

FIG. 13. Calculated ratio of the cross to diagonal peak intensities $R(x)$ as a function of the normalized mixing time $x=\Omega_0\tau_m$ in the case of a distribution of relaxation rates $T_1^{-1}=[T_1(u)]^{-1}$. Random-bond–random-field model of the glass phase has been used with glass parameters $T_G=90$ K and $\tilde{\Delta}=0.35$. The curves are calculated for $T=30$ K. Different $T_1(u=0)$ values are taken as parameters and $\Omega_0^{-1}=4$ s is assumed. The $T_1(u=0)\to\infty$ curve recovers the results of a single constant T_1.

bonds and those with larger asymmetry have a larger weight in the sum, whereas in the case of a single constant T_1 they all appear with the same weight. The cross to diagonal peak intensity ratio $R(x)$ in the case of a distribution of relaxation rates is even smaller than in the case of a single constant rate and cannot account for our "ergodicity restoring" results, where for long mixing times in DRADA the cross to diagonal peak intensity ratio $R(\infty)$ becomes equal to one. Here it should be stressed also that in DRADA at $T=30$ K T_1 amounts approximately to 300 s and the $R(x)$ curve of Fig. 13 practically does not deviate from the $T_1(u=0)\rightarrow\infty$ curve.

[1]S. F. Edwards and P. W. Anderson, J. Phys. F **5**, 965 (1975).

[2]D. Sherrington and S. Kirkpatrick, Phys. Rev. Lett. **35**, 1972 (1975).

[3]M. Mezard, G. Parisi, N. Sourlas, G. Toulouse, and M. Virasoro, Phys. Rev. Lett. **52**, 1156 (1984).

[4]J. R. L. de Almeida and D. J. Thouless, J. Phys. A **11**, 983 (1978).

[5]S. Nagata, P. H. Keesom, and H. R. Harrison, Phys. Rev. B **19**, 1633 (1979).

[6]For an excellent review of experiments and theoretical concepts on spin glasses see K. Binder and A. P. Young, Rev. Mod. Phys. **58**, 801 (1986).

[7]C. A. M. Mulder, A. J. van Duyneveldt, and J. A. Mydosh, Phys. Rev. B **23**, 1384 (1981).

[8]R. Pirc, B. Tadić, and R. Blinc, Z. Phys. B **61**, 69 (1985).

[9]R. Pirc, B. Tadić, and R. Blinc, Phys. Rev. B **36**, 8607 (1987).

[10]A. Levstik, C. Filipič, Z. Kutnjak, I. Levstik, R. Pirc, B. Tadić, and R. Blinc, Phys. Rev. Lett. **66**, 2368 (1991).

[11]Z. Kutnjak, C. Filipič, A. Levstik, and R. Pirc, Phys. Rev. Lett. **70**, 4015 (1993).

[12]R. Blinc, J. Dolinšek, V. H. Schmidt, and D. C. Ailion, Europhys. Lett. **6**, 55 (1988).

[13]R. Blinc, J. Dolinšek, R. Pirc, B. Tadić, B. Zalar, R. Kind, and O. Liechti, Phys. Rev. Lett. **63**, 2248 (1989).

[14]J. Dolinšek, J. Mag. Res. **92**, 312 (1991).

[15]R. Kind, R. Blinc, J. Dolinšek, N. Korner, B. Zalar, P. Cevc, N. S. Dalal, and J. DeLooze, Phys. Rev. B **43**, 2511 (1991).

[16]R. Blinc, J. Dolinšek, and S. Žumer, J. Non-Cryst. Solids **131-133**, 125 (1991).

[17]C. Schmidt, B. Blumich, and H. W. Spiess, J. Magn. Reson. **79**, 269 (1988).

[18]S. Kaufmann, S. Wefing, D. Schaefer, and H. W. Spiess, J. Chem. Phys. **93**, 197 (1990).

[19]R. R. Ernst, G. Bodenhausen, and A. Wokaun, *Principles of Nuclear Magnetic Resonance in One and Two Dimensions* (Clarendon, Oxford, 1987), Chap. 6.3.

[20]V. H. Schmidt and E. Uehling, Phys. Rev. **126**, 447 (1962).

[21]J. L. Bjorkstam and E. A. Uehling, Phys. Rev. **114**, 961 (1959).

[22]T. Chiba, J. Chem. Phys. **41**, 1352 (1964).

[23]R. Blinc, D. C. Ailion, B. Gunther, and S. Žumer, Phys. Rev. Lett. **57**, 2826 (1986).

[24]D. Suter and R. R. Ernst, Phys. Rev. B **32**, 5608 (1985).

[25]N. Bloembergen, S. Shapiro, P. S. Pershan, and J. O. Artman, Phys. Rev. **114**, 445 (1959).

[26]R. Blinc and B. Žekš, *Soft Modes in Ferroelectrics and Antiferroelectrics* (North-Holland, Amsterdam, 1974), and references therein.

[27]K. Schmidt-Rohr and H. W. Spiess, Phys. Rev. Lett. **66**, 3020 (1991).

[28]J. L. Bjorkstam, Phys. Rev. **153**, 599 (1967).

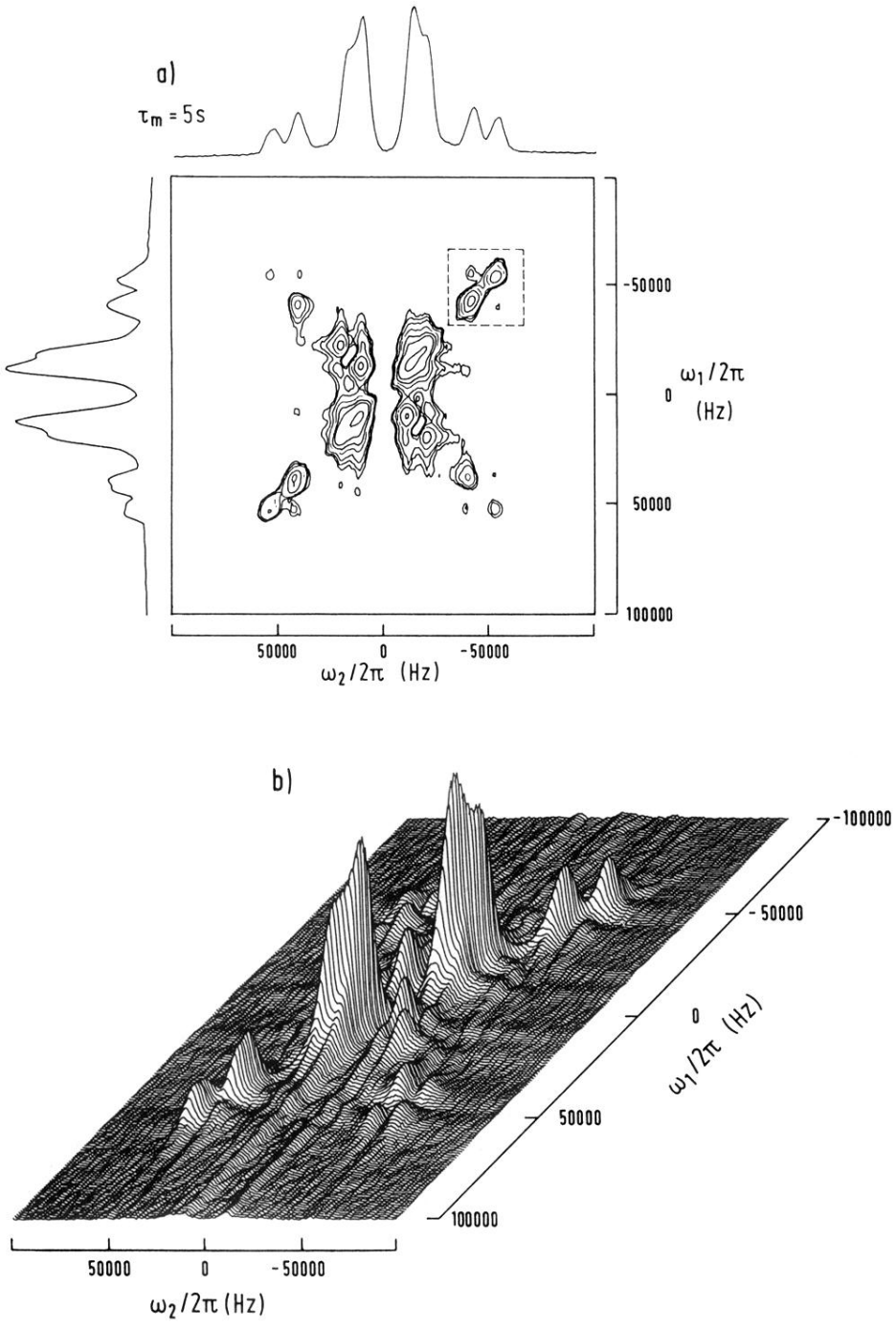

FIG. 6. (a) A 2D O-D. . . O deuteron exchange spectrum in DRADA $x=0.32$ at $T=40$ K, shown as a contour plot. The orientation is the same as that in Fig. 4 and the mixing time is $\tau_m=5$ s. The part of the spectrum, enclosed in a dashed box, corresponds to the $X_{\pm}$ bonds (lines A and B in Fig. 4). (b) Same spectrum displayed as a three-dimensional plot.

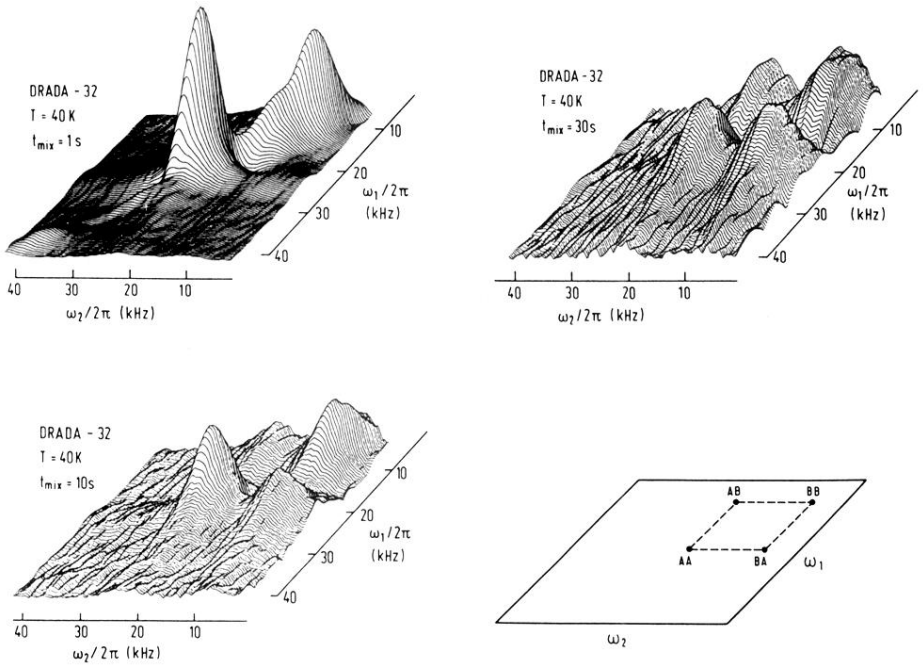

FIG. 7. O-D. . . O deuteron 2D exchange spectrum in DRADA $x=0.32$ at $T=40$ K for three different mixing times $\tau_m=1$, 10, and 30 s. Only the part of the spectrum corresponding to the X bonds [dashed box of Fig. 6(a)] is shown. At long mixing times cross peaks and diagonal peaks have the same intensities. In the lower right corner the assignation of the peaks in the 2D spectrum is shown.